United States Department of the Interior

Geological Survey

THERMAL REGIME OF PERMAFROST AT PRUDHOE BAY, ALASKA

by

Arthur H. Lachenbruch, J. H. Sass, B. V. Marshall, and T. H. Moses, Jr.

Open-File Report 82-535

1982

Abstract

Temperature measurements through permafrost in the oil field at Prudhoe Bay, Alaska, combined with laboratory measurements of the thermal conductivity of drill cuttings permit an evaluation of in situ thermal properties and an understanding of the general factors that control the geothermal regime. A sharp contrast in temperature gradient at ~600 m represents a contrast in thermal conductivity caused by the downward change from interstitial ice to interstitial water at the base of permafrost under near steady-state conditions. Interpretation of the gradient contrast in terms of a simple model for the conductivity of an aggregate yields the mean ice content (~39%), and thermal conductivities for the frozen and thawed sections (8.1 and 4.7 mcal/cm sec °C, respectively). These results yield a heat flow of ~1.3 HFU which is similar to other values on the Alaskan Arctic Coast; the anomalously deep permafrost is a result of the anomalously high conductivity of the siliceous ice-rich sediments. Curvature in the upper 160 m of the temperature profiles represents a warming of ~1.8°C of the mean surface temperature, and a net accumulation of 5-6 kcal/cm^2 by the solid earth surface during the last 100 years or so. Rising sea level and thawing sea cliffs probably caused the shoreline to advance tens of kilometers in the last 20,000 years, inundating a portion of the continental shelf that is presently the target of intensive oil exploration. A simple conduction model suggests that this recently inundated region is underlain by near-melting ice-rich permafrost to depths of 300-500 m; its presence is important to seismic interpretations in oil exploration and to engineering considerations in oil production. With confirmation of the permafrost configuration by offshore drilling, heat-conduction models can yield reliable new information on the chronology of arctic shorelines.

INTRODUCTION

Prudhoe Bay is a small embayment of the Alaskan Arctic Coast in the portion of the Arctic Ocean known as the Beaufort Sea (Figure 1). Since the discovery of large petroleum reserves there in the 1960's, it has been the site of intense geophysical exploration and of exploratory and production drilling. It lies at the northern edge of a treeless lake-strewn coastal plain in which the geomorphic characteristics of the surface and the thermal regime at depth are interrelated by the presence of permanently frozen sediment (permafrost) which typically extends to depths of hundreds of meters. Permafrost blocks the downward percolation of surface water, thereby contributing to the generally wet condition of the surface sediments and the abundance of standing bodies of water. Most of the processes that mold the natural landscape result from annual thawing and refreezing associated with the accumulation of solar heat by the wet surface, ponds, and rills, and the resulting collapse or flowage of the ice-rich materials. Similar processes can result in alteration of the terrain if the natural thermal regime is perturbed by engineering activity, e.g., the building of a roadway or heated structure, or the pumping of hot oil from a production well. For this reason, and for various scientific reasons as well, there is considerable interest in understanding the natural geothermal regime of the Prudhoe Bay area.

In coastal lowlands at high latitudes such as the Prudhoe Bay area, the geothermal regime differs from that in more familiar temperate latitudes in two important respects; one facilitates the interpretation and the other complicates it: 1) Because groundwater is generally immobilized in the cold permafrost (as ice) heat-conduction theory can usually be applied with confidence to within a few meters of the surface, 2) Because the mean annual temperature of the ground surface is ~10°C below the freezing point of water,

bodies of surface water such as lakes, rivers, and seas that do not freeze to the bottom (those deeper than ~2 m) represent hot spots on the surface that cause first-order perturbations to subsurface temperatures. Because of thermal interaction of the bodies of water with ice-rich permafrost on their shores, the sea in the Prudhoe Bay area presently encroaches on the land at rates on the order of 1 m/y, and the lakes grow, coalesce, migrate, and drain over periods $\sim 10^3$-10^4 years, leaving complicated three-dimensional transient geothermal disturbances in their wake. As a result of these effects, the mean annual temperature of the solid-earth surface (which is the boundary condition for geothermal models) may be strongly time- and position-dependent.

In this paper, we present thermal profiles through permafrost from several holes in an 800 km^2 land area adjacent to Prudhoe Bay. There are significant differences among these profiles associated with the variable surface conditions just discussed, and detailed study of these differences might yield useful information about the local geomorphic history of the surface [e.g., Lachenbruch, 1957; Lachenbruch et al., 1966]. Our purpose in this paper, however, is to explain the gross similarities in the profiles with a simple generalized one-dimensional model of the region. Such a model is useful for an understanding of regional conditions and for prediction of conditions where observations are not available. However, an awareness of the variable surface condition is necessary for an appreciation of the limitations of such a generalized model.

A complete one-dimensional description of the geothermal regime requires knowledge of the surface temperature and its recent variation with time, the heat flow from great depth, and the thermal conductivity and volumetric heat capacity of the earth materials. We shall attempt to estimate all of these

quantities from measurements of temperature in 14 holes drilled through permafrost, and from laboratory measurements of thermal conductivity of the mineral grains in drill-cuttings taken from some of these holes. The ice content of the permafrost and water content of the underlying sediments are inferred from analysis of the thermal disturbance caused by drilling and of the contrast in equilibrium thermal gradients at the base of permafrost. Thermal properties are then deduced with the additional information on grain conductivities and a model for the conductivity of an aggregate. The combined information permits a calculation of heat flow. The climatic warming of the last century or so is analyzed from data in the temperature profiles and the information on thermal properties.

Finally, we use the information on heat flow and thermal properties, and the knowledge that the Arctic shoreline is transgressing rapidly, to construct a simple model of transient thermal conditions in offshore permafrost; the on-shore model is used as an initial condition at the time of submergence. The results are useful for estimating the depth to the bottom of subsea permafrost in offshore regions with petroleum potential; conversely they may be used to reconstruct shoreline history if thermal information is obtained from offshore drilling.

MEASURED TEMPERATURES AND THE ESTABLISHMENT OF THERMAL EQUILIBRIUM

Figure 2 (modified from Gold and Lachenbruch, 1973) illustrates the contrasts and similiarities in generalized temperature profiles through permafrost at the four sites along the Alaskan Arctic Coast from which published data are available. The results from Cape Thompson are from Lachenbruch et al. [1966], from Cape Simpson the source is Brewer [1958], and from Barrow it is Lachenbruch et al. [1962]. The curve for Prudhoe Bay is a generalization of the data to be discussed in this paper.

The temperature profiles from the Prudhoe Bay wells are shown individually in Appendix C; hole locations are shown on the map in Figure 1 and some basic information for each hole is summarized in Table 1. (This manuscript, without Appendix C, has been submitted for outside publication, Lachenbruch et al. [1982].) The general features of the undisturbed temperature in the region are revealed in Figure 3, which shows temperature profiles from the nine holes (listed in Table 2) in which the drilling disturbance was relatively unimportant (less than a few tenths °C) by the time of the last observation. Although these curves differ in detail, they are roughly parallel to one-another, and they have a conspicuous common feature; their gradients change abruptly at a depth of about 600 ±20 m and a temperature of -1 ±0.5°C. We believe that this gradient change represents the effect on thermal conductivity of the change from pores filled with ice (above 600± m) to pores filled with water (below 600± m). Much of our analysis rests on an interpretation of this gradient change. The next to the last column in Table 1 presents an estimate of the equilibrium depth to this gradient change, i.e., to the bottom of ice-rich permafrost. The last column is an estimate of the equilibrium depth to the 0°C isotherm, the formally defined base of permafrost. A second conspicuous feature of the profiles in Figure 3 is their curvature in the upper 200 m, a feature common to all of the curves in Figure 2. This curvature represents a systematic trend toward warmer surface temperatures during the last century or so.

Before proceeding with an analysis of these features, it is useful to consider the lingering disturbance to the temperatures caused by the drilling process. An understanding of this disturbance not only helps us identify the natural (undisturbed) temperature, but it also increases our understanding of the properties of the undisturbed formations.

As the Prudhoe Bay wells were generally drilled to depths ~3 km where the natural formation temperatures are high (~100°C), the average temperature of the circulating fluid (~30-40°C) was very much greater than the near-freezing formation temperatures in the upper 750 m where we obtained our measurements. Hence during drilling of these holes, heat is transferred from the drilling fluid to the wall rocks, causing a perturbation to the natural temperatures which decreases with radial distance from the borehole. At the conclusion of drilling when fluid circulation stops, the source stops and the anomalous heat is dissipated by radial heat conduction as the temperature at each depth slowly returns to its natural (pre-drilling) value. The analytical details of the drilling disturbance depend upon many parameters, and they are the subject of an extensive literature. However, very simple models are adequate for a general understanding of the important features of the drilling disturbance in ice-rich permafrost.

These features are illustrated by the series of profiles taken at successive times after the completion of drilling in hole F (Figure 4). (Similar profiles from the Canadian Arctic can be seen in the extensive compilations by Taylor and Judge [1974, 1975, 1976, 1977] and Judge et al. [1979, 1981]. The duration of the heat source at any depth is normally the time elapsed from when the bit penetrates to that depth until circulation stops at the conclusion of drilling. We denote this time by s; for the data illustrated in Figure 4, $s \cong 44$ days for all depths. The interval between the

cessation of circulation and the time of observation is denoted by t^*. This post-drilling period, measured in multiples of the source duration, is the dimensionless time of observation denoted by τ. Thus the profiles labeled $\tau = .11$ and $\tau = 24.4$ (Figure 4a) represent measurements made 5 days and 1074 days after completion of drilling, respectively. (The four earliest profiles in Figure 4a have been discussed previously by Howitt [1971].)

It has been shown [e.g., Bullard, 1947; Lachenbruch and Brewer, 1959] that for post-drilling times t^* that are large relative to the duration of drilling s, the temperature at any depth in a drill hole is given to a good approximation by

$$\theta(\tau) \cong A \, \ell n \, (1 + \frac{1}{\tau}) + \theta_\infty, \tag{1a}$$

$$\tau \equiv \frac{t^*}{s} \gtrsim \beta \tag{1b}$$

where $\theta(\tau)$ is the temperature observed at dimensionless time τ, θ_∞ is the undisturbed (pre-drilling) temperature, A is a constant, and β is some minimum value of τ required for the validity of (1a).

If the drilling process behaved as an idealized line source, liberating heat at the constant rate of Q units of heat per unit depth throughout the drilling period s, equations 1 would be valid for all τ (i.e., $\beta = 0$), and A would be given explicitly by

$$A = \frac{Q}{4\pi K} \tag{2}$$

where K is thermal conductivity of the formation. Although the actual rate of radial heat loss is not constant during the drilling process, equations (1) generally are successful because variations in source strength with time are of little consequence to observations made long after the source terminates [Lachenbruch and Brewer, 1959]. Thus after an initial period (β, equation 1b)

determined by the departure of the real drilling process from the constant-source model, a straight line of slope A is expected in a plot of borehole temperature versus $\ell n(1 + 1/\tau)$. The value of Q determined from (2) yields an estimate of the mean source strength during drilling, and extrapolation to $\ell n(1 + 1/\tau) = 0$ (i.e., to $\tau \to \infty$) yields an estimate of Θ_∞. Such plots are presented for selected depths for hole F in Figure 4b; there the sign of the abscissa is reversed for intuitive convenience; the slope is -A and temperature decreases to the right with increasing time.

The temperatures at 650 and 700 m, which are below permafrost, lie close to straight lines as predicted by (1); the slopes (-A) are about -4°C. The other curves in Figure 4b represent depths within ice-rich permafrost and for these the linear approximation (1a) is generally unsatisfactory. This is because the interstitial ice thawed by the drilling process, releases latent heat when it later refreezes around the borehole. Drilling heat is stored by thawing and released long after drilling ceases by refreezing, thereby violating the assumption that the heat source vanishes at the conclusion of drilling. For the coldest permafrost (at a depth of 100 m, Figure 4b) refreezing is completed in less than one-half a drilling period ($\tau < 0.5$). Hence for the larger values of τ, refreezing behaves as a minor perturbation there, and the linear relation, with a slope similar to that at 700 m, is eventually recovered. In the warmer permafrost below 100 m refreezing takes longer, and much longer post-drilling times are required before equation (1a) can be applied for extrapolation. At the depth of the base of ice-rich permafrost (~600 m, Figure 4), a special situation occurs. There the equilibrium temperature is equal to the freezing temperature and refreezing may never be complete, but the equilibrium temperature is approached very much faster than at any other depth as can be seen in Figure 4a. This useful

fact can be explained by reference to the schematic representations in Figure 5.

In Figure 5, the dashed line "F.P." represents the freezing point of interstitial ice (the existence of a freezing interval is neglected), and the dotted line is the natural undisturbed formation temperature θ_∞. The relative values of F.P. and θ_∞ are different for measurements made within permafrost (Figure 5a), at the base of permafrost (Figure 5b), and below permafrost (Figure 5c). The abscissa represents radial distance from the borehole, the curve $\tau=0$ is the temperature disturbance at the conclusion of drilling, and the curves τ_1, τ_2 are radial temperature profiles at subsequent times. Within permafrost and below it (Figures 5a and c) we are dealing with a radial temperature disturbance that extends virtually to infinity. For such conditions, the approach to equilibrium generally requires a cooling interval very much larger than the source duration, i.e., equation (1a) requires

$$\tau \gg 1 \tag{3}$$

At the base of permafrost, however, the natural formation temperature (θ_∞) is the freezing temperature, and consequently the temperature disturbance cannot extend into the formation beyond the finite radius R of the region thawed around the borehole (Figure 5b). Hence for this case the return to equilibrium temperatures (though not in general to the frozen condition) is governed by the decay of an initial temperature in a cylinder of finite radius R with its lateral surface maintained at zero temperature. For such conditions, an initial axial temperature of a few tens of degrees would generally be reduced to a few tenths of degrees when the time t* satisfied

$$t^* \gtrsim \frac{\rho c R^2}{K} \tag{4}$$

[see e.g., Carslaw and Jaeger, 1959, Figure 12] where ρc is heat capacity per

unit volume of the thawed permafrost. The radius R may be estimated by equating the heat released by drilling, Qs, with the latent heat absorbed by the thawed cylinder, i.e.,

$$Qs = \pi R^2 \phi L \tag{5a}$$

where L is the latent heat per unit volume of ice, and ϕ is porosity. Substituting Q from equation (2), we obtain

$$R^2 \sim \frac{4KAs}{\phi L} \tag{5b}$$

Now combination of (4) and (5b) yields the equilibrium condition:

$$\tau \equiv \frac{t^*}{s} \gtrsim \frac{4\rho cA}{\phi L} \tag{6}$$

Substituting the values

$L \sim 73$ cal/cm^3

$\phi \sim 0.4$

$\rho c \sim 0.7$ cal/cm^3 °C

$A \sim 4°$ (from Figure 4b)

we obtain from (6)

$$\tau \gtrsim 0.4 \tag{7}$$

Comparing (7) to (3) we expect equilibration at the base of ice-rich permafrost to be an order of magnitude faster than at points distant from the base. Although the analysis leading to (7) is a gross idealization, it is seen from Figures 4a and 4b that the disturbance at $\tau \sim 1$ near the base of permafrost (at 600 m) is only a few tenths of a degree whereas at the same time it is a few degrees at smaller and greater depths. This very rapid approach to equilibrium at the base of ice-rich permafrost provides a useful

means of estimating permafrost depth, and (with a rough estimate of mean surface temperature) geothermal gradients, from disequilibrium thermal data.

It is clear from the foregoing analysis that the behavior of the decaying drilling disturbance is dominated by the effects of refreezing of interstitial ice at depths above ~600 m; at greater depths such effects are absent. This provides strong confirmation for the inference that the sharp change in gradient at ~600 m in the Prudhoe Bay wells results from the contrast in thermal conductivity between interstitial ice (above 600± m) and interstitial water (below 600± m). This interpretation is generally consistent with the fact that pure water at a depth of 600 m freezes at approximately -0.5°C under a hydrostatic load (ρ = 1 gm/cm^3), and at approximately -1.0°C under a lithostatic load (ρ = 2 gm/cm^3). Shortly after the completion of drilling, the axial temperature at the depth of gradient change is substantially higher (Figure 4) because of the persistance of radial temperature gradients. As equilibrium is approached, somewhat lower temperatures (to -1.5°C in hole A, Figure 3) probably result from a finite freezing interval associated with effects of locally increasing pressure, capillary forces, and/or small amounts of dissolved salts.

GRADIENT CONTRAST AT THE BASE OF PERMAFROST; IMPLICATIONS FOR ICE CONTENT

We have shown that it is likely that the region of low gradient above 600 ± 20 m (Figure 3) represents permafrost in which the interstitial moisture is predominantly in the form of ice; at greater depth the moisture is probably in the form of liquid water. If this is so, thermal balance at the base of the ice-rich layer (which, in general, will be moving with some velocity v) is given by

$$G_{th} K_{th} - G_{fr} K_{fr} = L\phi v \qquad (8)$$

where G represents thermal gradient, K represents thermal conductivity, and the subscripts "th" and "fr" refer respectively to material below the interface (thawed) and above the interface (frozen). As in equation (5), L is latent heat of melting per unit volume of ice, and ϕ is porosity (assumed to be the same as ice content). The right side of (8) represents the rate of absorption of heat at the interface if permafrost is thinning at the rate v; it must be balanced by the difference between heat conducted upward toward, and upward away from, the interface (left side of (8)). If the permafrost is neither thinning nor thickening, then $v \cong 0$, and the heat flow q is continuous across the interface. For this steady-state condition, (8) yields

$$q = G_{th} K_{th} = G_{fr} K_{fr} \qquad (9a)$$

$$\frac{G_{th}}{G_{fr}} = \frac{K_{fr}}{K_{th}} \qquad (9b)$$

We shall assume that the simple condition described by (9) obtains, and justify the assumption <u>a posteriori</u> by its implications.

Equation (9) describes the change from low gradient G_{fr} in permafrost to high gradient G_{th} beneath, caused by a change from high conductivity K_{fr} in

permafrost to low conductivity K_{th} beneath. If the only generally significant difference between the two materials is the state of their moisture, then the conductivity contrast is a consequence of the fact that ice is about four times as conductive as water. Hence the magnitude of the gradient contrast is a function of the fraction of water or ice present, which under the existing conditions of saturation is approximately equal to the porosity ϕ. An expression for the porosity ϕ in terms of the conductivity contrast of an aggregate in the frozen and thawed states is presented in Appendix A. We repeat the important results below.

Using the approximation [see Sass et al., 1971] that the conductivity of a saturated aggregate is the geometric mean of the conductivities of its constituents, we obtain for the frozen material

$$K_{fr} = K_i^{\phi} K_g^{1-\phi} \tag{10}$$

where K_i is the conductivity of ice (~5.45 cal/cm sec °C) and K_g is the mean conductivity of the mineral grains. They are evaluated at a reference temperature of -5°C, a reasonable average for the permafrost section. Similarly, the conductivity of the thawed material is given by

$$K_{th} = K_w^{\phi} (\gamma K_g)^{1-\phi} \tag{11}$$

where K_w is the conductivity of water (~1.34 cal/cm sec °C) at a reference temperature of +2°C and γ(~.983) adjusts K_g measured at the frozen reference temperature (-5°C) to the appropriate value at +2°C. Dividing equation (10) by (11), replacing the conductivity ratio by the gradient ratio with equation (9b), solving for ϕ, and inserting the numerical values yields (see equation A-12)

$$\phi = 0.722 \left\{ \ell n \frac{G_{th}}{G_{fr}} - 0.013 \right\} \tag{12}$$

Equation (12) is represented graphically in Figure 6. It permits us to estimate in situ porosity from the observable ratio of gradients measured within and below permafrost. The most important assumptions about the materials are that they are generally uniform except for the state of their interstitial moisture, and that the amount of unfrozen water in the frozen section is negligible (see Appendix A). These assumptions are believed to be reasonable in the relatively uniform coarse-grained sediments in the upper 750 m at Prudhoe Bay.

In the fifth and sixth column of Table 2, average thermal gradients have been estimated for the frozen and thawed portions of the nine holes for which near-equilibrium measurements were available. Their ratio is shown in the seventh column and the value of porosity calculated with equation (12), in the eighth. The values are high with a range about 30%-45% and a mean of 38.5%; they agree well with direct measurements made on frozen core from a hole in which no temperatures were recorded (see Appendix B).

ESTIMATION OF THERMAL CONDUCTIVITY AND HEAT FLOW

It is seen from equations (10) and (11) that with the porosity Φ known, the individual conductivities of the frozen and thawed sections can be estimated from a knowledge of the average grain conductivity K_g. The relationship is illustrated in Figure 7 for selected values of grain conductivity (K_g at the temperature of the frozen material, and γK_g at the temperature of the thawed material). For a given porosity (abscissa), the conductivities in the frozen and thawed states are given by the solid and dashed curves, respectively.

We measured the grain conductivities by the method of Sass et al. [1971] on 46 samples of cuttings representing the upper 750 m in holes A, C, and M. The values are surprisingly uniform (columns 9 and 10, Table 2), and averages for each hole do not differ significantly from the average for all measurements which is 10.24 cal/cm sec °C; no systematic variation with depth was found. (These values of grain conductivity contain a small adjustment for the difference between the temperature of the measurement apparatus and the reference temperature of -5°C selected for the analysis of frozen samples (see Appendix A).) The values for conductivity of permafrost (column 11, Table 2) and the underlying thawed material (column 12, Table 2) were calculated for each hole from equations (10) and (11) using the mean value of K_g (column 10, Table 2) and the values of ϕ obtained from (12) (column 8, Table 2). The mean values so obtained for conductivity of permafrost and the underlying material are ~8.1 and ~4.7 mcal/cm sec °C, respectively (columns 11, 12, Table 2). They are represented by dots in Figure 7 to permit a visual estimate of the sensitivity of these results to errors in K_g or ϕ.

The last column of Table 2 shows the heat flow calculated for each hole using equation (9a) and the tabulated values for gradient (column 6) and conductivity (column 11). From these values we select a best estimate of 1.3 HFU with an uncertainty conservatively estimated as ±0.2 HFU.

MEAN ANNUAL SURFACE TEMPERATURE AND ITS CHANGE IN THE LAST CENTURY

We have mentioned that the departure of the generalized temperature profiles shown in Figure 2 from linearity in the upper 200 m is the effect of a systematic change in the heat balance at the earth's solid surface during the last 100 years or so. The data from Cape Thompson [Figure 2 and Lachenbruch et al., 1966] suggest an increase in mean annual surface temperature of 1.5-2°C during this event, and the site analyzed near Barrow yields an increase about twice as great [Figure 2 and Lachenbruch et al., 1962; Gold and Lachenbruch, 1973]. Unfortunately the data from Prudhoe Bay (Figure 3) are not well-suited for the study of climatic change because of their variability in the upper 200 m; we believe that most of this variability results from the local three-dimensional transient effects of variable surface conditions discussed in the introduction. Nevertheless most of the Prudhoe Bay profiles show a marked curvature in the upper portion, with near-surface temperatures significantly warmer than those obtained by upward extrapolation of the generalized gradient (G_{fr}). We have attempted to characterize this curvature in columns 2, 3, and 4 of Table 2.

The second column in Table 2 gives our estimate of the surface intercept of the extrapolated gradient G_{fr}, allowing for the drilling disturbance where appropriate. The mean value of ∿-10.9°C can be viewed as the average surface temperature with which the deep permafrost is presently in equilibrium. The fourth column gives an estimate of the depth at which the measured profiles depart from the linear extrapolation from depth. The departure of the two curves represents the heat accumulated by the earth during the recent climatic warming; it has penetrated to an estimated average depth of ∿160 m (column 4, Table 2). The average departure at a depth of 50 m is estimated to be ∿1°C (column 3, Table 2). As the present-day gradient is generally negligible in

the upper 50 m and the extrapolated gradient is 16°C/km (0.8°C per 50 m) we estimate that the present mean surface temperature exceeds the temperature at which the permafrost equilibrated by an average value of about 1.8°C. In summary, we deduce that the mean surface temperature in the area increased from a previous stable value averaging about -10.9 to the present value averaging about -9.1°C, and that the effect of the warming has penetrated about 160 m into the earth. From these data, we should like to estimate the duration of the warming episode and the magnitude of the flux imbalance at the earth's surface responsible for it. For this purpose, we shall use a simple conduction model that we have applied previously [e.g., Lachenbruch et al., 1966]. Because of the current interest in contemporary climatic change, and to correct an error in a previous discussion [equation 17, Gold and Lachenbruch, 1973], we shall present a more detailed discussion than might otherwise be warranted by the quality of the data from Prudhoe Bay.

We shall assume that the increase in mean ground surface temperature T(0,t) can be represented by an expression of the form

$$T(0,t) = Dt^{\frac{n}{2}} , \qquad 0 < t < t_o \tag{13}$$

where D is a constant, n can be any positive integer (or zero), and t is time since the start of the warming; $t = t_o$ represents the present day and t_o is the duration of the warming event. Thus if the earth materials are homogeneous, the transient departure of the temperature profile from its steady-state

configuration at any depth z is [Carslaw and Jaeger, p. 63, 1959]

$$\frac{T(z,t)}{T(0,t)} = 2^n \Gamma(\tfrac{1}{2}n+1)\ i^n \mathrm{erfc}\frac{z}{\sqrt{4\alpha t}} \tag{14a}$$

$$= \mathrm{erfc}\frac{z}{\sqrt{4\alpha t}}\ , \qquad n = 0 \tag{14b}$$

$$= \sqrt{\pi}\ i\ \mathrm{erfc}\frac{z}{\sqrt{4\alpha t}}\ , \quad n = 1 \tag{14c}$$

$$= 4\ i^2\ \mathrm{erfc}\frac{z}{\sqrt{4\alpha t}}\ , \quad n = 2 \tag{14d}$$

where $\alpha = K/\rho c$ is thermal diffusivity and $i^n\mathrm{erfc}\beta$ is the nth repeated integral of the error function of β [e.g., Appendix II, Carslaw and Jaeger, 1959]. Differentiation of (14) yields the instantaneous flux imbalance f(t) at the earth's surface at time t.

$$f(t) = \frac{\Gamma(\frac{1}{2}n+1)}{\Gamma(\frac{1}{2}n+\frac{1}{2})} \frac{K}{\sqrt{\alpha t}}\ T(0,t) \tag{15a}$$

$$= \frac{1}{\sqrt{\pi}} \frac{K}{\sqrt{\alpha t}}\ T(0,t) \qquad , n = 0 \tag{15b}$$

$$= \frac{\sqrt{\pi}}{2} \frac{K}{\sqrt{\alpha t}}\ T(0,t) \qquad , n = 1 \tag{15c}$$

$$= \frac{2}{\sqrt{\pi}} \frac{K}{\sqrt{\alpha t}}\ T(0,t) \qquad , n = 2 \tag{15d}$$

Integration of (15) yields the average instantaneous flux imbalance ($\bar{f}(t_o)$, from the start of the warming (t = 0) to the present ($t = t_o$)

$$\bar{f}(t_o) = \frac{2}{n+1}\ f(t_o) \tag{16}$$

Equation 16 is valid for any non-negative integral value of n.

It is seen from (13) that the case n=0 represents a step increase in surface temperature at time t=0, n=2 represents surface temerature increasing linearly with time. Similarly (13) and (15c) show that the case n=1 represents a step increase in heat flux at the surface at time t=0; for n>1 flux increases with time, for n<1 it decreases with time. Where precise temperature observations are available in homogeneous permafrost materials, it is, in principle, possible to select the best-fitting value of n in (13) from a comparison of the observed disturbance and that calculated from (14) [see e.g., Lachenbruch et al., 1966], or even to infer a more refined representation of surface temperature change by superimposing results from several terms like that in (13) [see Gold and Lachenbruch, 1973; Birch, 1948]. This is possible because the recent warming is conspicuous and easily identified in superficial thermal profiles and because the usual thermo-hydrologic complications in such measurements can be neglected with confidence in cold permafrost.

In the present case we do not have detailed information on the form of the disturbance, $T(z,t_o)$, with depth, but only estimates of two parameters: the total temperature change $T(0,t_o)$ at the surface at time t_o, and the depth z^* at which the present temperature change $T(z^*,t_o)$ is negligible. These data can be used to obtain rough estimates of the duration of the recent warming and the magnitude of the unbalanced flux for simple assumed forms of the climatic change (n=0, 1, and 2, equation 16). From the foregoing discussion, we start with

$$T(0,t_o) \cong 1.8°C \tag{17}$$

$$\frac{T(z^*,t_o)}{T(0,t_o)} = \varepsilon << 1 \quad , \quad z^* \gtrsim 160 \text{ m} \tag{18}$$

The conductive time constant $\lambda(z^*)$, a rough estimate of the time required for a surface disturbance to penetrate to depth z^*, is given by

$$\lambda(z^*) = \frac{z^{*2}}{4\alpha} \tag{19a}$$

$$\cong 127 \text{ yrs if } z^* = 160 \text{ m}, \alpha = 0.016 \text{ cm}^2/\text{sec} \tag{19b}$$

The value of diffusivity in (19b) is obtained from the value of $K_{fr} \sim 0.008$ cal/cm sec °C (Table 2) and $\rho c \cong 0.5$ cal/cm² °C. Thus it is likely that the observed disturbance is largely a product of the last century. For a more refined estimate of t_o we set $\varepsilon \cong 0.05$ in (18), corresponding to our estimate that the undetected disturbance at 160 m is ~0.1°C and obtain from equations (14):

$$t_o \cong 67 \text{ yrs} \quad n = 0 \tag{20a}$$

$$\cong 90 \text{ yrs} \quad n = 1 \tag{20b}$$

$$\cong 117 \text{ yrs} \quad n = 2 \tag{20c}$$

The average unbalanced heat flux at the surface for the three models is (equations 15 and 17)

$$\bar{f}(t_o) \cong 90 \text{ cal/cm}^2/\text{yr} \quad n = 0 \tag{21a}$$

$$\cong 60 \text{ cal/cm}^2/\text{yr} \quad n = 1 \tag{21b}$$

$$\cong 45 \text{ cal/cm}^2/\text{yr} \quad n = 2 \tag{21c}$$

And the total heat accumulation per square centimeter of earth's surface during the entire event for all three cases is (equations 20 and 21)

$$t_o \bar{f}(t_o) \cong 5400 \pm 10\% \text{ cal/cm}^2 \tag{22}$$

Thus the conspicuous warming (most easily discussed in terms of n=1) is equivalent to a net accumulation of heat by the earth at a rate sufficient to melt only 0.8 cm of ice annually (21b) for the past 90 years (20b), about three orders of magnitude less than the heat absorbed and re-radiated annually by the earth's surface. This unbalanced influx is of the same order of magnitude (though opposite in sign) as the steady heat flow from the earth's interior (1.3 HFU $\cong$ 41 cal/cm^2/yr, see column 13, Table 2).

THE CAUSE OF ANOMALOUSLY DEEP PERMAFROST AT PRUDHOE BAY

Inspection of Figure 2 suggests that the permafrost is anomalously deep at Prudhoe Bay in comparison to the other sites along the Alaskan Arctic Coast. To investigate why this is so, we represent the depth to the bottom of permafrost, Z, by the approximate relation

$$Z \cong K_{fr} \frac{(-\theta_o)}{q}$$

where θ_o is the long-term mean surface temperature (in °C) obtained by upward extrapolation. Low heat flow, q, low surface temperature, θ_o, and high conductivity, K_{fr}, favor deep permafrost, Z. The heat flow at Cape Thompson is 1.4 HFU [Lachenbruch et al., 1966], not appreciably different from the value of 1.3 HFU that we have herein determined for Prudhoe Bay, and the heat flow at Barrow has been estimated to be in the same range [Lachenbruch and Brewer, 1959]. Hence the variations in permafrost thickness on the Alaskan Arctic Coast are probably controlled largely by variations in surface temperature and conductivity. Permafrost is much deeper at Prudhoe Bay than at Cape Thompson because the mean surface temperature is much lower there (∿-11°C at Prudhoe Bay; ∿-7°C at Cape Thompson); thermal conductivity of the silicious siltstone at Cape Thompson is ∿7 mcal/cm sec °C which is almost as great as K_{fr} at Prudhoe Bay (Table 2). By contrast, permafrost is much deeper at Prudhoe Bay than at Barrow and Simpson in spite of the lower θ_o (∿-12°C) at the latter sites. Clearly the deeper permafrost at Prudhoe Bay is the effect of a much higher thermal conductivity there (K_{fr} ∿8 mcal/cm sec °C). The permafrost at Barrow and Simpson is argillaceous and fine grained; at Prudhoe Bay, it is silicious and coarse grained. The two reasons for lower conductivity at Barrow and Simpson are 1) argillaceous grains have lower conductivities (K_g) than siliceous grains, and 2) in fine-grained sediments

capillary forces inhibit the formation of interstitial ice (see Appendix A). The second point is confirmed at Cape Simpson by the uniformity of the observed geothermal gradient across the base of permafrost there (Figure 2 and Brewer [1958]).

DEPTH OF ICE-RICH PERMAFROST BENEATH PRUDHOE BAY - A SIMPLE MODEL

At Prudhoe Bay, and many other portions of the Arctic Coast of North America, the shoreline has been rapidly encroaching on the land as a combined effect of the eustatic rise in sea level of the past 20,000 years [Hopkins, 1982], and of the thermal erosion of vulnerable permafrost banks along the shore. Consequently, much of the terrain that is presently submerged beneath the edge of the ocean was, only a few thousand years ago, part of the land and was exposed to the same rigorous climate that resulted in the deep permafrost described in the foregoing sections. Although the sea bed is much warmer than the land surface, permafrost that formed prior to submergence may persist at great depths beneath the sea for many thousands of years. With the reasonable assumption that geothermal conditions beneath the submerged portion of the Prudhoe Bay region were the same prior to submergence as they are on land today, it is possible to use the foregoing results to construct a simple model for the depth of permafrost after submergence. A model of this kind, or parts of it, have been suggested in the past [e.g., Terzaghi, 1952; Mackay, 1972; Hunter et al., 1976; Sharbatyan and Shumskiy, 1974). The situation at Prudhoe Bay is unique, however, because there we have determined all of the parameters necessary to obtain applicable numerical results. For this reason, we present a fairly explicit, if idealized, account of the model. (For a more elaborate version accounting for sedimentation and thawing at the sea bed, see Lachenbruch and Marshall [1977].) The problem is of interest because its solution provides a means of reconstructing shoreline history from thermal measurements in offshore boreholes, and because it provides information needed for the interpretation of seismic surveys and for the solution of engineering problems associated with development of the petroleum resource in permafrost beneath the edge of the Arctic Ocean.

As a starting point, we consider the model illustrated in Figure 8. Just prior to submergence, the temperature is represented by the curve t = 0, the parameters for which we generalize from the data presented above:

θ_o = extrapolated mean temperature at the surface z = 0 (-10.9°C, Table 2) (23a)

Z(0) = depth to the base of ice-rich permafrost (600 ± m, Table 1) (23b)

θ_b = temperature at the base of ice-rich permafrost (-1± °C, Figure 3) (23c)

At time t = 0, we suppose that the ocean overrode the site in question and in a relatively short time the mean annual surface temperature rose from θ_o, characteristic of the land, to a value θ_s, characteristic of the sea bed. Except for a narrow band near the beach where sea ice freezes to the bottom, or where brines accumulate beneath sea ice [see e.g., Osterkamp, 1975/1976; Osterkamp and Harrison, 1976], the minimum sea bed temperature is about -1.8°C, the freezing temperature of normal sea water. This temperature obtains during most of the year because the shallow water is usually covered by floating ice; for brief ice-free periods in summer the water and sea bed may be considerably warmer. Hence in the Prudhoe Bay area θ_s is typically in the range -1.3 ± 0.5 °C [see e.g., Lachenbruch and Marshall, 1977], very close to the value θ_b (equation 23c) at the base of permafrost. (This fact will permit us to neglect their difference below, thereby simplifying the analysis.) Therefore, submergence is followed by a period in which the 'triangular cold-reserve 'of Figure 8 is depleted by rapid conduction of heat downward from the warm sea bed at z = 0, and by continued influx of geothermal heat from below (at z = Z). Stages in this process are shown schematically by the curves in Figure 8 representing successive times t_1, t_2, and t_3 after submergence. When the time reaches t_3, the cold reserve is essentially depleted, and temperatures throughout permafrost are close to its freezing point because the boundary temperatures θ_s and θ_b are. From this time onward,

the warm ice-rich permafrost thins progressively from below owing to the melting by geothermal heat accumulating at z = Z. (Some downward melting from the sea bed also occurs; it is sensitive to the value of θ_s, sedimentation and erosion on the sea bed, and the salinity and mass transport of interstitial water in the sediments. These processes, which have been discussed in detail by W. H. Harrison and T. E. Osterkamp and their colleagues at the University of Alaska, are complicated and incompletely understood; we shall not address them here [see Harrison and Osterkamp, 1978; Lachenbruch and Marshall, 1977; Sellman and Chamberlain, 1980].)

Thus the thinning of ice-rich sub-sea permafrost from below involves two stages 1) the depletion of the cold reserve (i.e., the input of the sensible heat required to raise its temperatures to near-melting), and 2) the subsequent steady melting from below by geothermal heat.

To investigate the duration of the first stage, we make the simplifying assumption that the permafrost thickness Z does not diminish appreciably during the depletion of the cold reserve, i.e., that $Z(0) \cong Z(t_3)$, Figure 8. (The error in this assumption will be estimated later.) We, therefore, solve the problem illustrated by the right-hand drawing of Figure 9a: find the temperature θ in a slab of constant thickness Z(0) with basal temperature θ_b if it is initially in equilibrium with a surface temperature θ_o and that temperature is suddenly raised to θ_s at time t = 0. The solution is the sum of a transient part θ_1 and a steady-state part θ_2 illustrated in Figure 9a and described as follows:

$$\theta(z,t) = \theta_1(z,t) + \theta_2(z) \quad , \quad 0 \leqq z \leqq Z \tag{24}$$

where $$\theta_2 = \theta_s + (\theta_b - \theta_s)\frac{z}{Z} \tag{25}$$

and θ_1 is the solution to the differential equation

$$\frac{\partial\theta_1}{\partial t} = \alpha\frac{\partial^2\theta_1}{\partial z} \quad , \quad 0 \leqq z \leqq Z \tag{26a}$$

subject to the conditions

$$\theta_1(z,0) = (\theta_o - \theta_s)\,(1 - \frac{z}{Z}) \quad , \quad t = 0 \tag{26b}$$

$$\theta_1(z,t) = 0 \quad , \quad z = 0 \text{ and } Z \, , \quad t > 0 \tag{26c}$$

Here α is thermal diffusivity of the frozen sediments; it is related to thermal conductivity K, specific heat c, and density ρ by

$$\alpha = \frac{K}{\rho c} \tag{26d}$$

The solution to equations 26 is

$$\theta_1(z,t) = (\theta_o - \theta_s)\,\frac{2}{\pi}\sum_{n=1}^{\infty}\frac{1}{n}\,e^{\frac{-n^2\pi^2}{4}\frac{t}{\lambda}}\sin(n\pi\,\frac{z}{Z}) \tag{27}$$

where the time constant λ is given by

$$\lambda = \frac{Z^2}{4\alpha} \tag{28a}$$

$$\cong 1800 \text{ years for Prudhoe Bay} \tag{28b}$$

The numerical value in (28b) is obtained from the values $Z \cong 600$ m, $\alpha \cong 0.016$ cm^2/sec, determined previously for the frozen sediments at Prudhoe Bay (see equations 19b and 23b).

Results from equation (27) are shown graphically in Figure 9b where it is seen that for times exceeding one time constant (~1800 years for Prudhoe Bay) the subfreezing cold-reserve inherited by inundated permafrost is virtually depleted.

To estimate the rate of upward thinning of permafrost, we assume that the unfrozen region below remains in a quasi steady-state during the process, and consequently the heat supplied to the base of permafrost at Z(t) remains

constant and equal to the geothermal flux q. Heat balance at the base then requires (see equation 8)

$$-L\phi\frac{dZ}{dt} \cong q - K_{fr}\frac{d\theta}{dz} \quad , \qquad \text{(29a)}$$

$$\cong q - K_{fr}\frac{d\theta_1}{dz} - K_{fr}\frac{\theta_b - \theta_s}{Z(t)} \qquad \text{(29b)}$$

$$\Big\} \quad z = Z(t)^-$$

where (29b) is obtained by substitution of (24) and (25). It can be seen from Figure 9b, or equation 32 below that for $t > \lambda$ the derivative on the right in (29b) is small, and as we have mentioned, at Prudhoe Bay the third term on the right in (29b) is also generally small ($\theta_b \cong \theta_s$). Consequently after the first 1800 years or so the base of permafrost rises approximately as

$$\frac{-dZ}{dt} \cong \frac{q}{L\phi} \quad , \quad t > \lambda \cong 1800 \text{ years} \qquad \text{(30a)}$$

$$\cong 1.46 \text{ cm/yr} \qquad \text{(30b)}$$

where the numerical value in (30b) is obtained from

$$q = 1.30 \text{ HFU } (= 41 \text{ cal/cm}^2 \text{ yr}), \text{ Table 2} \qquad \text{(31a)}$$

$$\phi = 0.385, \text{ Table 2} \qquad \text{(31b)}$$

$$L = 73 \text{ cal/cm}^3 \qquad \text{(31c)}$$

Thus after the initial stage of warming, i.e., after the first 1800± yrs, the base of ice-rich permafrost will rise at the rate of about 1.5 cm/yr.

We now return to the problem of how much the base of permafrost might rise during the initial stage, during which time the derivative in (29b) cannot be neglected. Its value, obtained from differentiation of (27) is

$$\left.\frac{d\theta_1}{dz}\right|_{Z^-} = (\theta_o - \theta_s)\frac{2}{Z}\sum_{n=1}^{\infty}(-1)^n e^{\frac{-n^2\pi^2}{4}\frac{t}{\lambda}} \qquad \text{(32)}$$

Substituting (32) in (29b), neglecting the third term on the right in (29b) as before, and integrating yields an estimate of the decrease in permafrost

thickness $\Delta Z(t)$ during an initial warming period of duration t.

$$\Delta Z(t) = \frac{1}{L\phi} \{qt - K_{fr} \frac{\theta_s - \theta_o}{Z} \frac{2}{3} \lambda [1 + \frac{12}{\pi^2} \sum_{n=1}^{\infty} \frac{(-1)^n}{n^2} e^{\frac{-n^2\pi^2}{4} \frac{t}{\lambda}}]\} \qquad (33a)$$

which is valid as long as

$$\Delta Z << Z \qquad (33b)$$

For $t \gtrsim \lambda$, the series in (33a) can be neglected. Consequently, the rise in the base of permafrost for an initial period of duration λ is given approximately by

$$\Delta Z(\lambda) \cong \frac{\lambda}{L\phi} \{q - \frac{2}{3} K_{fr} \frac{\theta_s - \theta_o}{Z}\} \qquad (34a)$$

This result may be simplified without appreciable error at Prudhoe Bay by replacing θ_s by θ_b in which case the second term in braces is simply 2/3 q and (34) becomes

$$\Delta Z(\lambda) \cong \frac{1}{3} \lambda \frac{q}{L\phi} \qquad (34b)$$

$$\cong 9 \text{ meters at Prudhoe Bay} \qquad (34c)$$

The numerical value (34c) justifies the assumption (33b). Comparing (34) and (30), we see that the average rate in rise of the base of ice-rich permafrost during an initial period with a duration of one time constant, is about 1/3 of the subsequent rate of rise. This is a fairly general rule which will usually be applicable to other arctic coastal localities with different initial temperatures and properties as long as the ice content ϕ is sufficiently large that $\Delta Z(t=\lambda)$ in equation (33a) satisfies (33b).

In summary, we can generalize the foregoing results to form a rule of thumb: Following rapid submergence in the Prudhoe Bay area, the base of permafrost will generally rise about 10 m (from a depth of about 600 m) during

the first 2000 years, and thereafter it will rise about 15 meters per 1000 years. This estimate should remain valid until the permafrost gets so thin ($\lesssim$100 m) that the distinction between θ_s and θ_b, and details of heat and mass transfer at the sea bed begin to influence conditions at the lower boundary of permafrost [Lachenbruch and Marshall, 1977]. According to this rule, ice-rich permafrost extending to a depth of 500 m beneath the sea bed would be expected to persist 8,000 years after submergence; after 20,000 years, the depth would still be over 300 m. In applying this rule, it is necessary to recall the assumptions of the model from which it was derived. The most important are: 1) at the time of inundation (t=0) the surface temperature changed instantaneously from θ_o, characteristic of land, to θ_s characteristic of the seabed where the water is deep enough ($\gtrsim$2 m) to prevent sea ice from freezing to it, and 2) the subsurface temperature and lithology beneath the seabed at the time of submergence were the same as they are beneath the adjacent land today.

Estimates of contemporary transgression rates [Barnes et al., 1977; Hopkins and Hartz, 1978] taken with the sea level history reconstructed by Hopkins [1982] suggest that shoreline transgression probably proceeded at rates of ~1-10 m/yr for the past 15,000-20,000 years. As the present seabed slopes gently (~1 m/km) out to ~50 km from shore near Prudhoe Bay, this suggests that the time required for the sea to obtain a depth $\gtrsim$2 m ranged from a few centuries to a few thousand years. During this period, the surface temperature would undergo a transition from θ_o to θ_s, and the time origin for application of the rule should be chosen with this in mind. A second point regarding the choice of time origin relates to local conditions within Prudhoe Bay proper, which is a small closed topographic basin (Figure 1) and might have been occupied by a lake prior to encroachment of the sea. If this is so, the time of inundation there should be reckoned from the time of formation of

the lake; this could add many thousands of years to the time available for the degradation of permafrost at this locality. Superficial thermal measurements (to ~20 m) beneath the seabed within Prudhoe Bay proper support this ancestral lake hypothesis [Lachenbruch and Marshall, 1977]. More generally, if thermal measurements are made in offshore holes being drilled for petroleum exploration, they can be used with models of the type presented here to obtain reliable information on the history of the Arctic shoreline.

The second question regarding application of the above rule of thumb concerns how much of the presently submerged continental shelf was exposed to the permafrost-producing climate long enough to generate the initial condition that we have assumed; the problem has been discussed by Mackay [1972]. According to Hopkins [1982], sea level in the Beaufort Sea probably stood at least 25 m below its present level between about 10,000 and 75,000-80,000 years before present. Under reasonable climatic assumptions, this provides sufficient time for the portion of the shelf exposed during that period to develop a thermal regime similar to our initial condition. If the solid surface of the shelf had the same configuration as it has today, the rule of thumb would be applicable at least to a distance of 25 km from the present shoreline; this includes much of the area presently under study as a potential petroleum resource. However, the seabed elevation has been modified by sedimentation, and degradation of permafrost, and the sea level history is uncertain. Consequently, refinement of our estimates of the offshore distribution of permafrost and of the geomorphic history of the continental shelf of the Beaufort Sea must await additional thermal and stratigraphic information to be obtained from offshore drilling.

SUMMARY

We have made repeated measurements of temperature to depths of about 750 m in holes drilled on land within about 20 km of Prudhoe Bay on the Alaskan Arctic Coast, and measurements of the thermal conductivity of sediment grains recovered from some of those holes. From these two types of measurements, we have attempted to characterize the geothermal regime of the region and the major processes that control it.

Analysis of repeated temperature measurements in individual holes reveals that the dissipation of the temperature disturbance due to drilling is dominated by the effects of latent heat of refreezing interstitial water at depths less than 600 ± 20 m (depending on the hole); at greater depths, such effects are absent. This implies that high porosity ice-rich permafrost extends to depths of 600± m. Analysis of equilibrium thermal profiles reveals a sharp increase in thermal gradient at these depths (from ~16°C/km above to ~28°C/km below). These observations suggest that the gradient contrast is caused by the contrast in thermal conductivity resulting from pores filled with ice above 600± m and pores filled with water below. Equilibrium temperatures of -1 ± 0.5 °C observed at these depths are consistent with this view. If we assume that the permafrost is not thinning or thickening and that its unfrozen moisture content is negligible, it is possible to apply a model for the thermal conductivity of an aggregate to obtain a formula (12) that yields the in situ porosity ϕ from a knowledge of the contrasting thermal gradients; no knowledge of the thermal conductivity is required. The average porosity so obtained is 38.5%. With the in situ porosity known, it is only necessary to determine the average conductivity of the mineral grains to calculate the in situ thermal conductivity of the frozen and thawed materials

(the conductivities of ice and water are known). From our laboratory measurements of grain conductivities on samples from some of the observation holes, we calculated mean thermal conductivities of 8.1 and 4.7 mcal/cm sec °C for the frozen and thawed portions of the section respectively. With the thermal conductivity and thermal gradient known, the steady heat flow from the earth's interior can be calculated. Its value is 1.3 ± 0.2 HFU, a value typical of stable continental regions [Lachenbruch and Sass, 1977].

The foregoing estimates of in situ porosity, conductivity, and heat flow are based on the validity of our model for the thermal conductivity of an aggregate (Appendix A) and the assumptions that the permafrost is in a thermal steady state and that its unfrozen moisture content is negligible. The porosities calculated on the basis of these assumptions agree with porosities measured on natural-state frozen core samples from the area, and thermal conductivities measured on such samples in both the frozen and thawed state show satisfactory agreement with values calculated by our model (Appendix B). These observations tend to confirm the assumptions and lend confidence to the conclusions based upon them.

With a general knowledge of the thermal properties and heat flow in the Prudhoe Bay region, it is possible to investigate some of the physical processes that control the thermal regime there. Neither the mean surface temperature nor the heat flow at Prudhoe Bay are anomalous for the Alaskan Arctic Coast and consequently the anomalously deep permafrost is a consequence of the high thermal conductivity of the coarse-grained siliceous ice-rich sediments there. As has been found elsewhere on the Alaskan Arctic Coast, anomalously warm temperatures in the upper 160 m of permafrost represent a sharp climatic warming during the past 100 years or so. At Prudhoe Bay, we

estimate that it represents a total increase in mean ground surface temperature of ~1.8°C (from -10.9 to -9.1), and a net absorption of heat by the solid earth of 5000-6000 cal/cm^2 during the event.

The present rate of retreat of the shoreline at Prudhoe Bay due to degradation of permafrost banks is ~1 m/yr [Hopkins and Hartz, 1978; Barnes et al., 1977] and at times during the past 20,000 years it might have been an order of magnitude greater as a result of eustatic rise in sea level. If the inundated terrain initially had a thermal regime like that we observe on land today, we can estimate geothermal conditions beneath the recently submerged portions of the continental shelf. It will generally take about 2000 years after rapid submergence for the initially cold permafrost to approach the near-melting sea-bed temperature. During this time, the permafrost, initially extending to a depth of about 600 m, will thin only about 10 m from below. Thereafter the warmed permafrost would thin from the bottom at the rate of about 15 m/1000 years. Hence even after 8000 years of submergence, ice-rich permafrost would extend to a depth of ~500 m, and after 15,000 years to ~400 m. Thus deep ice-rich permafrost at near-melting temperatures (and hence vulnerable to engineering disturbance) is expected throughout extensive near-shore regions that are currently of interest in connection with petroleum exploration. If measurements of subsea temperatures are made during offshore exploration, they may be interpreted in terms of heat-conduction models to provide a new source of information on the chronology of Arctic shorelines.

Acknowledgments. We are grateful to BP Alaska, Inc., and the Atlantic Richfield Company for their helpful cooperation and assistance in obtaining the temperature measurements upon which this paper is based. In particular, we should like to acknowledge the help provided by Kaye Howard of BP Alaska,

Inc., and Jerry A. Rochon of ARCO. We also thank BP Alaska, Inc., for providing us with frozen core samples from boring 12-10-14, and for allowing us to use their comprehensive report on the engineering properties of the core. We are grateful for helpful reviews of our manuscript by T. E. Osterkamp, W. D. Harrison, Marianne Guffanti, and Manuel Nathenson. We also thank our colleagues, Eugene P. Smith and Robert J. Munroe, for performing conductivity tests on the core and cuttings and for assistance with data reduction.

References

Barnes, Peter, Erk Reimnitz, Greg Smith, and John Melchior, Bathymetric and shoreline changes, northwestern Prudhoe Bay, Alaska, Open-file Rep. 77-161, U.S. Geol. Surv., Menlo Park, California, 15 pp., 1977.

Birch, F., The effects of Pleistocene climatic variations upon geothermal gradients, Am. J. Sci., 246, 729-760, 1948.

Birch, F., and H. Clark, The thermal conductivity of rocks and its dependence on temperature and composition, Am. J. Sci., 238, 529-558 and 613-635, 1940.

Brewer, M. C., Some results of geothermal investigations of permafrost in northern Alaska, Trans. Am. Geophys. Union, 39, 19-26, 1958.

Bullard, E. C., The time necessary for a borehole to attain temperature equilibrium, Mon. Not. Roy. Astron. Soc. Geophys. Suppl., 5, 127-130, 1947.

Dorsey, N. E., Properties of Ordinary Water-Substance, Reinhold Publishing Corporation, New York, 1940.

Gold, L. W., and A. H. Lachenbruch, Thermal conditions in permafrost--A review of North American literature, Proceedings of the Second International Conference on Permafrost, Yakutsk, July 1973, North American Contribution, pp. 3-25, Nat. Acad. of Sci., Nat. Res. Counc., Washington, D. C., 1973.

Harrison, W. D., and T. E. Osterkamp, Heat and mass transport processes in subsea permafrost, 1. An analysis of molecular diffusion and its consequences, J. Geophys. Res., 83, 4707-4712, 1978.

Hopkins, D. M., Aspects of the paleogeography of Beringia, in Paleogeography of Beringia, edited by D. M. Hopkins, J. V. Matthews, Jr., C. E. Schweger, and S. B. Young, Academic Press, in press, 1982.

Hopkins, D. M., and R. W. Hartz, Coastal morphology, coastal erosion, and barrier islands of the Beaufort Sea, Alaska, Open-file Rep. 78-1063, U.S. Geol. Surv., Menlo Park, California, 54 pp, 1978.

Howitt, Frank, Permafrost geology at Prudhoe Bay, World Petroleum, 42, 28-38, 1971.

Hunter, J. A. M., A. S. Judge, H. A. MacAulay, R. L. Good, R. M. Gagne, and R. A. Burns, The occurrence of permafrost and frozen sub-seabottom materials in the southern Beaufort Sea, Beaufort Sea Proj. Tech. Rep. 22, Dep. of the Environment, Victoria, B. C., 1976.

Judge, A. S., A. E. Taylor, and M. Burgess, Canadian geothermal data collection - Northern wells, 1977-78, Can. Dep. Energy, Mines Resour., Earth Phys. Branch, Geothermal Series, 11, 187 pp., 1979.

Judge, A. S., A. E. Taylor, M. Burgess, and V. S. Allen, Canadian geothermal data collection - Northern wells, 1978-80, Can. Dep. Energy, Mines Resour., Earth Phys. Branch, Geothermal Series, 12, 190 pp., 1981.

Lachenbruch, A. H., Thermal effects of the ocean on permafrost, Bull. Geol. Soc. Am., 68, 1515-1530, 1957.

Lachenbruch, A. H., and M. C. Brewer, Dissipation of the temperature effect of drilling a well in Arctic Alaska, U.S. Geol. Surv. Bull. 1083-C, 73-109, 1959.

Lachenbruch, A. H., M. C. Brewer, G. W. Greene, and B. V. Marshall, Temperatures in permafrost, in Temperature--Its Measurement and Control in Science and Industry, vol. 3, part 1, pp. 791-803, Reinhold, New York, 1962.

Lachenbruch, A. H., G. W. Greene, and B. V. Marshall, Permafrost and the geothermal regimes, in Environment of the Cape Thompson Region, Alaska, edited by N. J. Wilimovsky and J. N. Wolfe, pp. 149-163, U.S. Atomic Energy Comm., Div. Tech. Inf., 1966.

Lachenbruch, A. H., and B. V. Marshall, Sub-sea temperatures and a simple tentative model for offshore permafrost at Prudhoe Bay, Alaska, Open-file Rep. 77-395, U.S. Geol. Surv., Menlo Park, California, 1977.

Lachenbruch, A. H., and J. H. Sass, Heat flow in the United States and the thermal regime of the crust, in The Earth's Crust, Geophys. Monogr. Ser., vol. 20, edited by J. G. Heacock, pp. 626-675, AGU, Washington, D. C., 1977.

Lachenbruch, A. H., J. H. Sass, B. V. Marshall, and T. H. Moses, Jr., Permafrost, heat flow, and the geothermal regime at Prudhoe Bay, Alaska: J. Geophys. Res., in press, 1982.

Mackay, J. R., Offshore permafrost and ground ice, southern Beaufort Sea, Canada, Can. J. Earth Sci., 9, 1550-1561, 1972.

Osterkamp, T. E., A conceptual model of offshore permafrost, North. Engineer, 7, 5-10, Winter 1975-1976.

Osterkamp, T. E., and W. D. Harrison, Subsea permafrost, Its implications for offshore resource development, North. Engineer, 8, 31-35, 1976.

Sass, J. H., A. H. Lachenbruch, and R. J. Munroe, Thermal conductivity of rocks from measurements on fragments and its application to heat-flow determinations, J. Geophys. Res., 76, 3391-3401, 1971.

Sass, J. H., A. H. Lachenbruch, R. J. Munroe, G. W. Greene, and T. H. Moses, Jr., Heat flow in the western United States, J. Geophys. Res., 76, 6376-6413, 1971.

Sellmann, P. V., and E. J. Chamberlain, Permafrost beneath the Beaufort Sea: Near Prudhoe Bay, Alaska, J. Energy Resour. Technol., 102, 35-48, 1980.

Sharbatyan, A. A., and P. A. Shumskiy, Extreme estimations in geothermy and geocryology, USACRREL Draft Translation 465, 140 pp., 1974.

Taylor, A. E., and A. S. Judge, Canadian geothermal data collection - Northern wells, 1955 to February 1974, Can. Dep. Energy, Mines Resour., Earth Phys. Branch, Geothermal Series, 1, 171 pp., 1974.

Taylor, A. E., and A. S. Judge, Canadian geothermal data collection - Northern wells, 1974, Can. Dep. Energy, Mines Resour., Earth Phys. Branch, Geothermal Series, 3, 127 pp., 1975.

Taylor, A. E., and A. S. Judge, Canadian geothermal data collection - Northern wells, 1975, Can. Dep. Energy, Mines Resour., Earth Phys. Branch, Geothermal Series, 6, 142 pp., 1976.

Taylor, A. E., and A. S. Judge, Canadian geothermal data collection - Northern wells, 1976-77, Can. Dep. Energy, Mines Resour., Earth Phys. Branch, Geothermal Series, 10, 194 pp., 1977.

Terzaghi, K., Permafrost, J. Boston Soc. Civ. Engineers, 39, 30-31, 1952.

Walsh, J. B., and E. R. Decker, Effect of pressure and saturating fluid on the thermal conductivity of compact rock, J. Geophys. Res., 71, 3053-3061, 1966.

Woodside, W., and J. H. Messmer, Thermal conductivity of porous media, J. Appl. Phys., 32, 1688, 1961.

TABLE 1. Basic Data and Permafrost Depth

Well designation									
This paper	Company	N. Lat.	W. Long.	Elev. (m)	Duration of drilling (days)	No. of logs	τ for last log	Depth of ice (m)	Depth to 0°C (m)
A	BP 33-12-13	70° 21.4'	148° 50.1'	5	51	3	27	620	660
B	BP 04-11-13	70° 19.8'	148° 50.8'	7	59	3	23	620	640
C	BP 19-10-15	70° 12.7'	148° 24.7'	16	39	3	38	570	595
D	BP 23-11-13	70° 17.7'	148° 45.1'	8	73	2+	18	605	---
E	ARCO NPBS 1	70° 22.7'	148° 31.6'	6	70	3	18	560	605
F	BP 8-11-13	70° 19.2'	148° 54.5'	10	44	10	24	600	620
G	BP 31-11-14	70° 16.1'	148° 40.4'	10	56	4	23	620	650
H	BP 11-11-13	70° 20.3'	148° 46.1'	5	48	1	2.1	620±	640±
I	BP 12-11-13	70° 20.3'	148° 46.1'	5	41	1	1.5	620±	640±
J	BP 1-11-13	70° 20.3'	148° 46.1'	5	46	1	0.1	610±	---
K	ARCO 1-5	70° 14.4'	148° 24.1'	15	32	1	7.22	600±	---
L	BP 31-10-16	70° 10.9'	148° 09.5'	10	155	1	1.6	590±	---
M	BP 27-11-14	70° 16.7'	148° 33.9'	8	130	2	5.5	580±	625
N	ARCO EBS 1	70° 18.7'	148° 18.9'	5	169	1	8.0	580±	625±
							Mean (±SD)	600 (±20)	630 (±20)

TABLE 2. Climatic change and heat-flow parameters from observation wells

(1)	(2)	(3)	(4)	(5)	(6)	(7)	(8)	(9)	(10)	(11)	(12)	(13)
	Climatic change parameters			Gradients (°C/km) (measured)			Porosity	K_g (-5°C) (meas.) (calc.)		Cond. (calculated)		Heat flow
Well designation	θ_o (extr)	$\Delta\theta$(50m)	Δz	G_{th}	G_{fr}	$\frac{G_{th}}{G_{fr}}$	ϕ	N	Mean [±Std. Er.]	K_{fr} (-5°)	K_{th} (+2°)	q (HFU)
A	-11.4	1.4	190	27	16	1.70	.370	12	10.30 [±0.43]	8.11	4.77	1.30
B	-11.1	1.1	150	30	16½	1.82	.419			7.86	4.32	1.30
C	- 9.8	0.5	140	27½	15½	1.77	.399	10	10.42 [±0.70]	7.96	4.50	1.23
D	-11.0	1.1	160	27½	17½	1.57	.313			8.41	5.35	1.47
E	-12.0	1.5	180	29	19	1.53	.294			8.51	5.56	(1.62)
F	-11.0	1.0	160	30	17	1.76	.395			7.98	4.54	1.36
G	-10.6	0.8	170	29	15	1.93	.462			7.65	3.96	1.15
M	-10.7	0.8	170	28½	15½	1.84	.427	24	10.14 [±0.26]	7.82	4.25	1.21
N	-10.6	0.5	150	25½	15½	1.65	.349			8.22	4.98	1.27
Mean	-10.91	0.97	163	28.2	16.4	1.73	0.385	46	10.24 [±0.23]	8.06	4.69	1.32
(±Std. Dev.)	(±.61)	(±0.36)	(±16)	(±1.5)	(±1.3)	(±0.13)	(±.057)		(±1.54)	(±0.28)	(±0.52)	(±.14)
											Neglecting Hole E	1.29 (±0.10)

Column (2) Extrapolated equilibrium surface temperature (prior to climatic change) (°C).

Column (3) Climatic temperature disturbance at 50 m (°C).

Column (4) Depth of climatic disturbance (meters).

Column (8) Porosity calculated from column (7) and equation 12.

Column (10) Mean [and standard error] of N measured values of grain conductivity K_g adjusted to -5°C (mcal/cm sec °C).

Columns (11) & (12) In situ conductivity calculated from columns (8) and (10) and equation (10) or (11).

Column (13) Heat flow in heat-flow units (10^{-6} cal/cm² sec) calculated from columns (6) and (11).

Illustrations

Figure 1. Map of the Prudhoe Bay area showing location of the wells described in Table 1 (dots) and of BP boring 12-10-14 (star) from which frozen core was obtained.

Figure 2. Generalized profiles of measured temperature on the Alaskan Arctic Coast (solid lines). Dashed lines represent extrapolations.

Figure 3. Near-equilibrium profiles from the nine holes from which they were available (see Table 2).

Figure 4. a) Successive temperature profiles from hole F observed from five days (τ = 0.11) to three years (τ = 24.4) after completion of drilling.

b) Representation of the dissipation of the drilling disturbance in hole F for selected depths indicated at right-hand margin. τ is time elapsed since completion of drilling measured in multiples of the drilling period s(= 44 days).

Figure 5. Schematic representation of the radial disturbance to formation temperatures at the completion of drilling (τ = 0) and at two subsequent times τ_1 and τ_2 (solid curves). F.P. is the freezing temperature of interstitial moisture (dashed line), and θ_∞ is the undisturbed pre-drilling temperature (dotted line). Parts a), b), and c) represent depths with equilibrium temperatures less than, equal to, and greater than the freezing point, respectively.

Figure 6. Idealized relation between porosity and the ratio of geothermal gradients from the frozen and thawed sections (equation 12). Dot represents point determined from the mean value of the ratio of observed gradients (Table 2).

Figure 7. Idealized relation for the thermal conductivity (K) of a saturated aggregate as a function of porosity (ϕ) for selected grain conductivities. Solid curves are for the frozen state (equation 10) with grain conductivity K_g. Dashed curves are for the thawed state (equation 11) with grain conductivity γK_g. Dots represent mean values from Table 2.

Figure 8. Schematic representation of the warming and thinning of ice-rich permafrost of thickness Z(t) after submergence at time t = 0. θ_b is the basal temperature, θ_o is the surface temperature prior to submergence, θ_s is the seabed temperature, and q is geothermal flux.

Figure 9. Model for the initial warming of permafrost after submergence (with thinning neglected). a) Decomposition into a steady-state part (θ_2) and transient part (θ_1), b) Analytical results for the transient part; λ is the time constant which is approximately 1800 years for conditions at Prudhoe Bay.

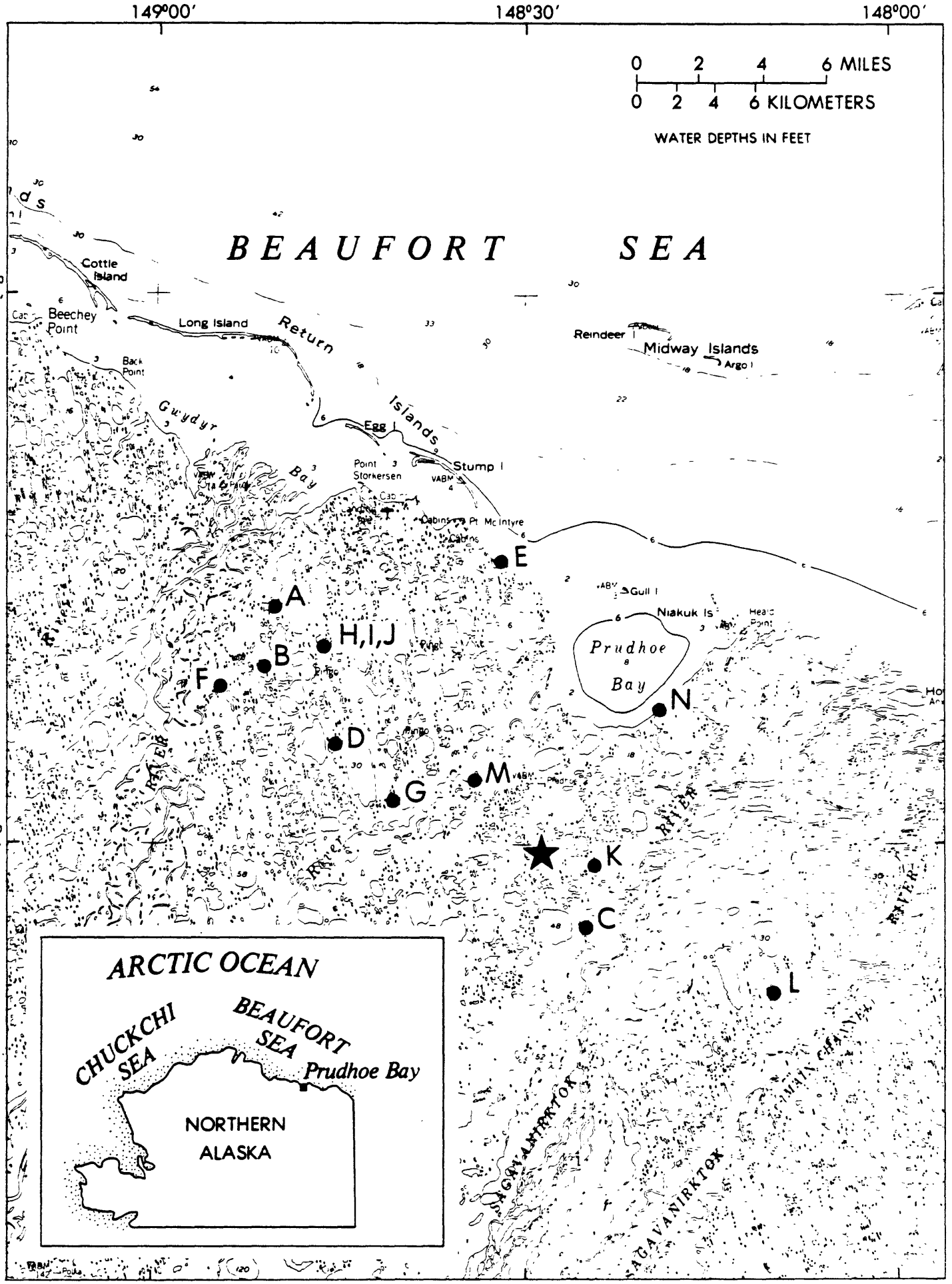
149°00′
148°30′
148°00′
0 2 4 6 MILES
0 2 4 6 KILOMETERS
WATER DEPTHS IN FEET
BEAUFORT SEA
70° 30′
70° 15′
Cottle Island
Beechey Point
Long Island
Return Islands
Reindeer I
Midway Islands
Argo I
Back Point
Gwydyr Bay
Egg I
Point Storkersen
Stump I
Cabins
Pt McIntyre
Gull I
Niakuk Is
Prudhoe Bay
A
B
C
D
E
F
G
H,I,J
K
L
M
N
ARCTIC OCEAN
CHUCKCHI SEA
BEAUFORT SEA
Prudhoe Bay
NORTHERN ALASKA

Figure 1

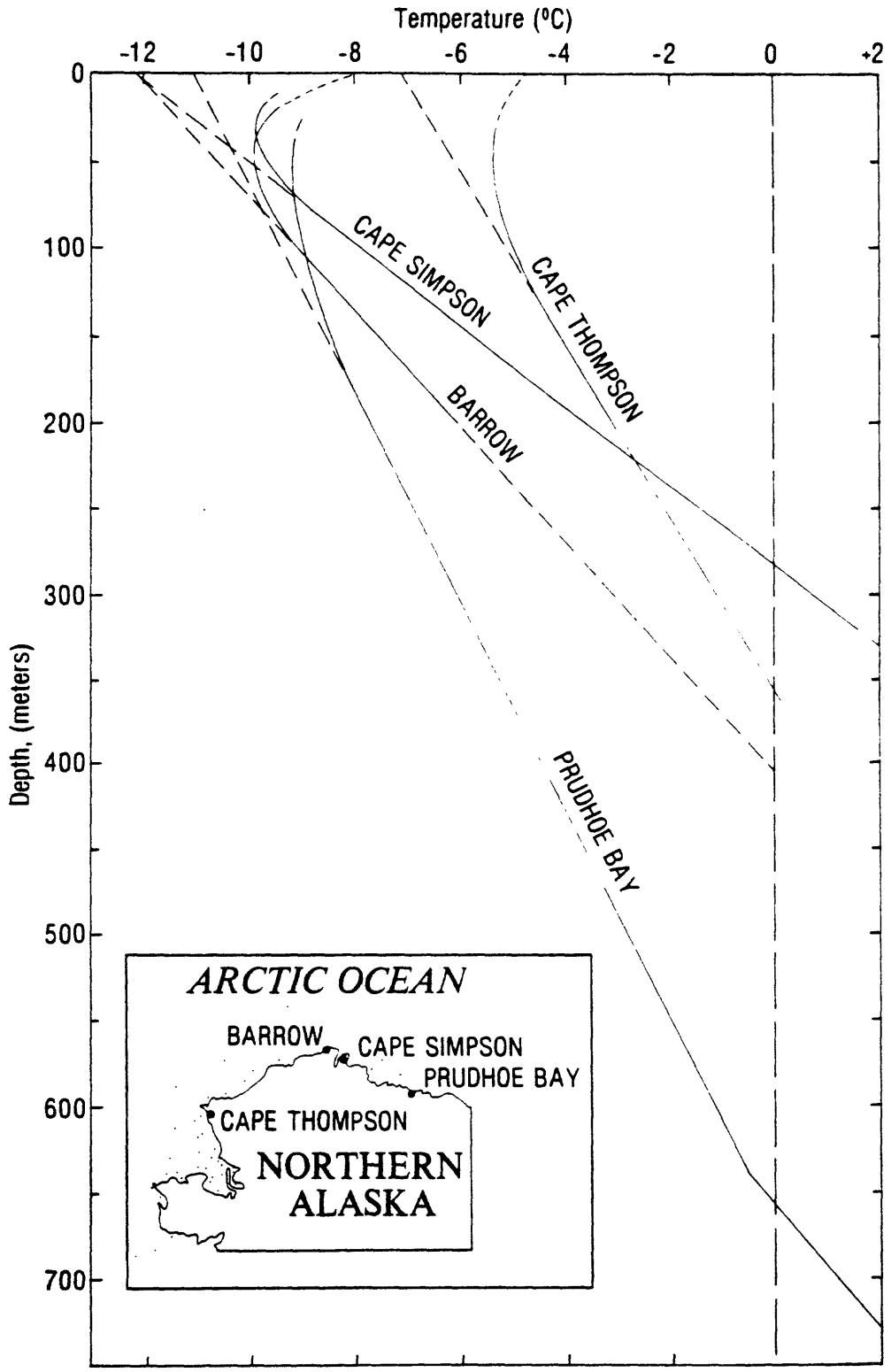
Temperature (°C)
-12
-10
-8
-6
-4
-2
0
+2
0
100
200
300
400
500
600
700
Depth, (meters)
CAPE SIMPSON
CAPE THOMPSON
BARROW
PRUDHOE BAY
ARCTIC OCEAN
BARROW
CAPE SIMPSON
PRUDHOE BAY
CAPE THOMPSON
NORTHERN ALASKA

Figure 2

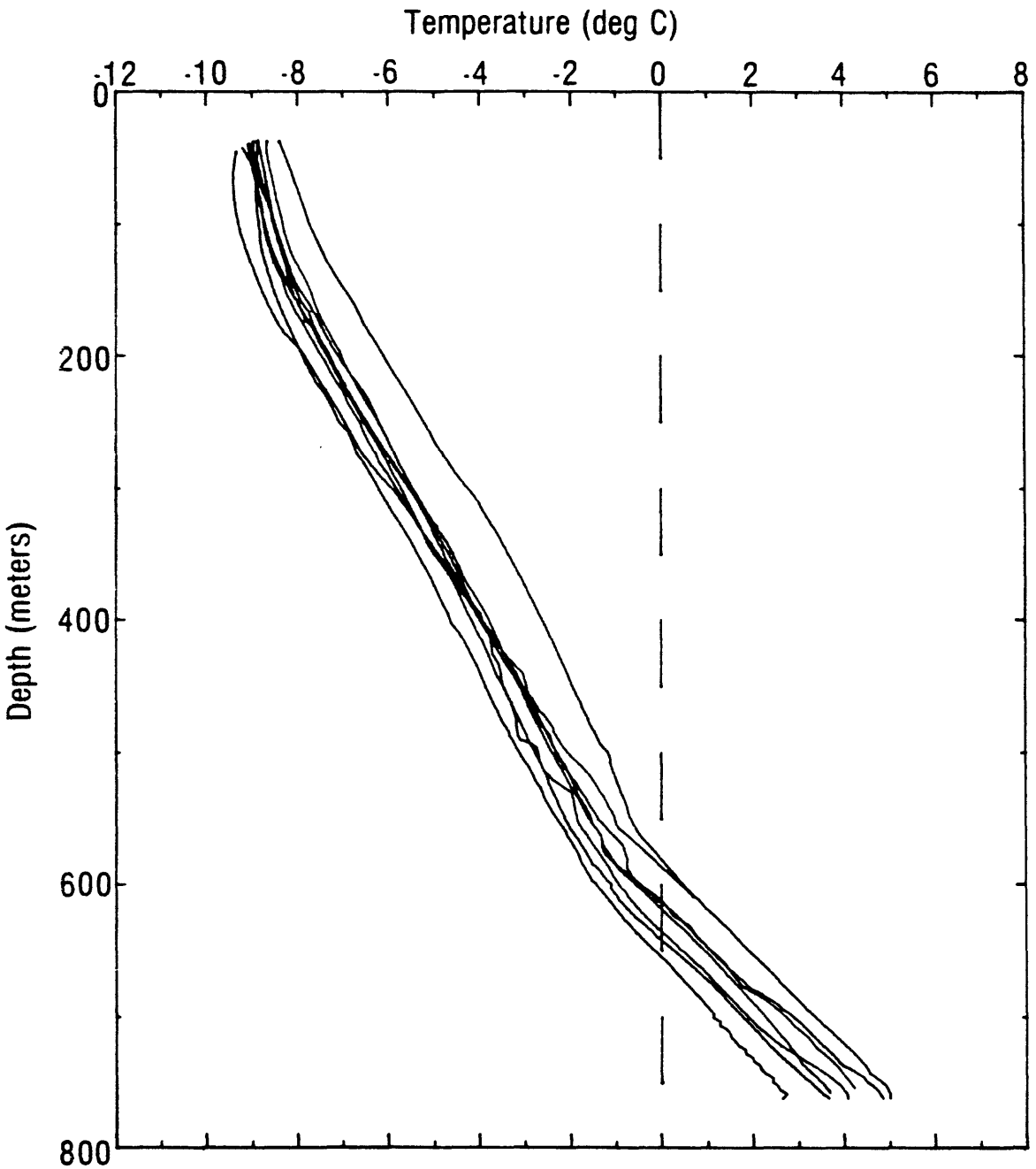
Temperature (deg C)
-12
-10
-8
-6
-4
-2
0
2
4
6
8
0
200
400
600
800
Depth (meters)

Figure 3

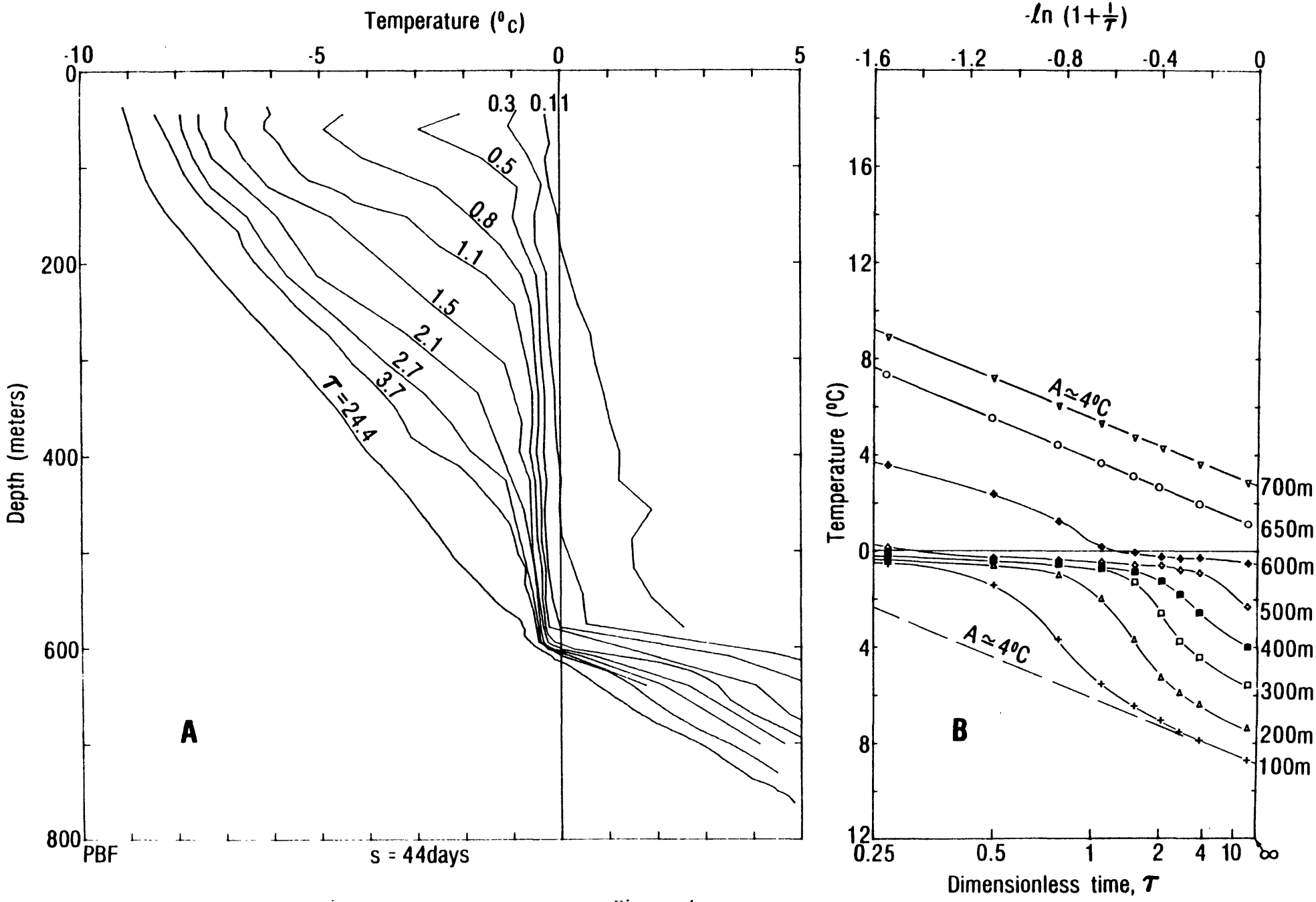
Temperature (°C)
-10
-5
0
5
0
200
400
600
800
Depth (meters)
0.3
0.1
1
0.5
0.8
1.1
1.5
2.1
2.7
3.7
τ=24.4
A
PBF
s = 44days
-ln (1+1/τ)
-1.6
-1.2
-0.8
-0.4
0
16
12
8
4
0
4
8
12
Temperature (°C)
A≃4°C
A≃4°C
B
700m
650m
600m
500m
400m
300m
200m
100m
0.25
0.5
1
2
4
10
∞
Dimensionless time, τ

Figure 4

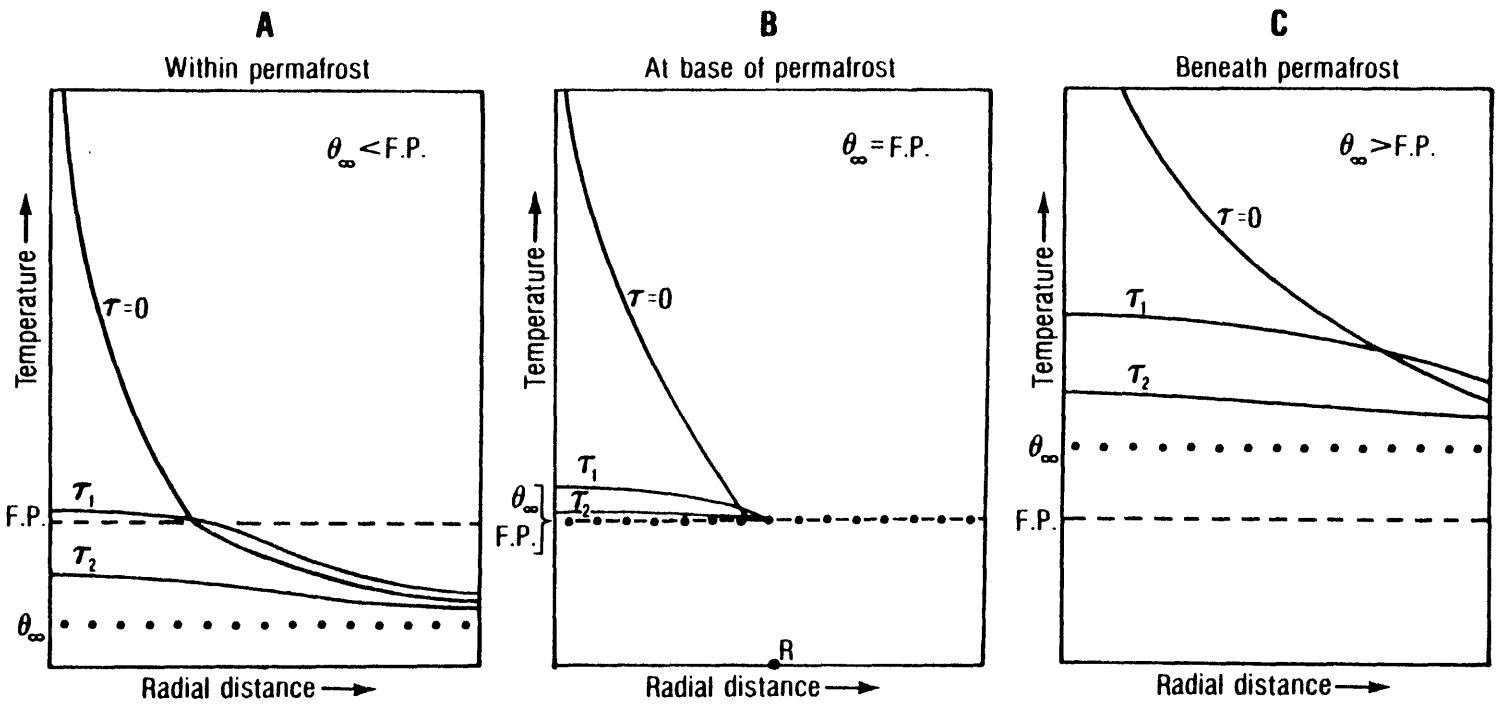
A
Within permafrost
θ_∞<F.P.
Temperature
τ=0
τ_1
F.P.
τ_2
θ_∞
Radial distance
B
At base of permafrost
θ_∞=F.P.
Temperature
τ=0
τ_1
θ_∞
τ_2
F.P.
R
Radial distance
C
Beneath permafrost
θ_∞>F.P.
Temperature
τ=0
τ_1
τ_2
θ_∞
F.P.
Radial distance

Figure 5

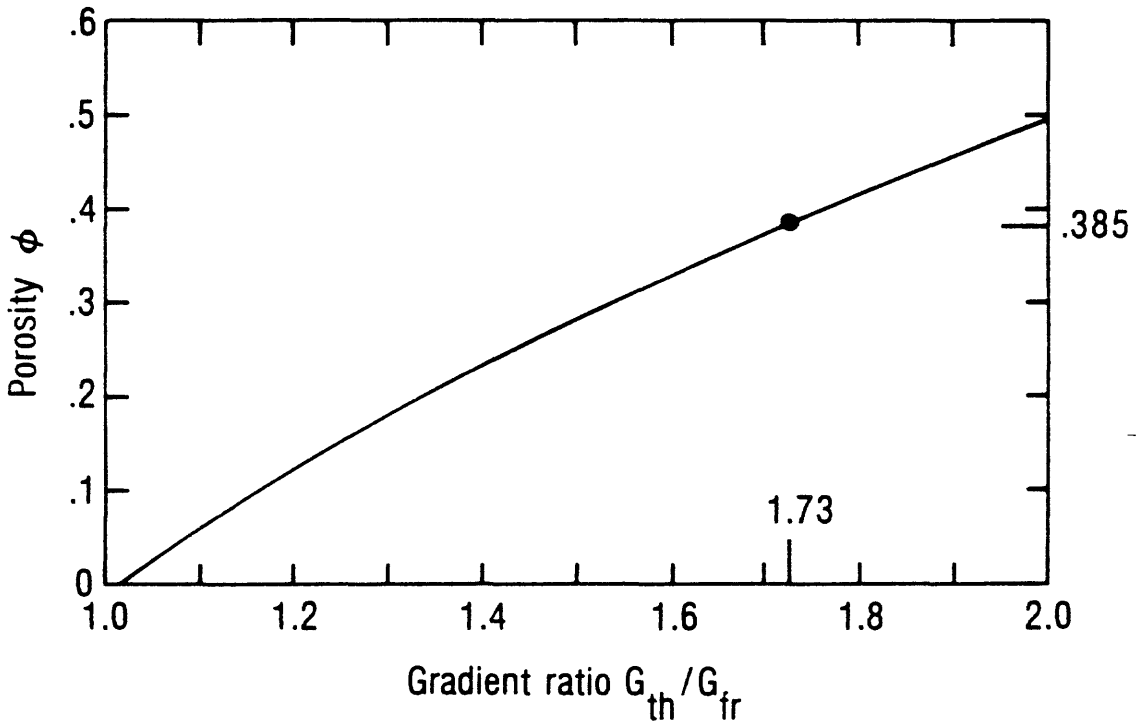
.6
.5
.4
.3
.2
.1
0
Porosity ϕ
.385
1.73
1.0
1.2
1.4
1.6
1.8
2.0
Gradient ratio G_{th}/G_{fr}

Figure 6

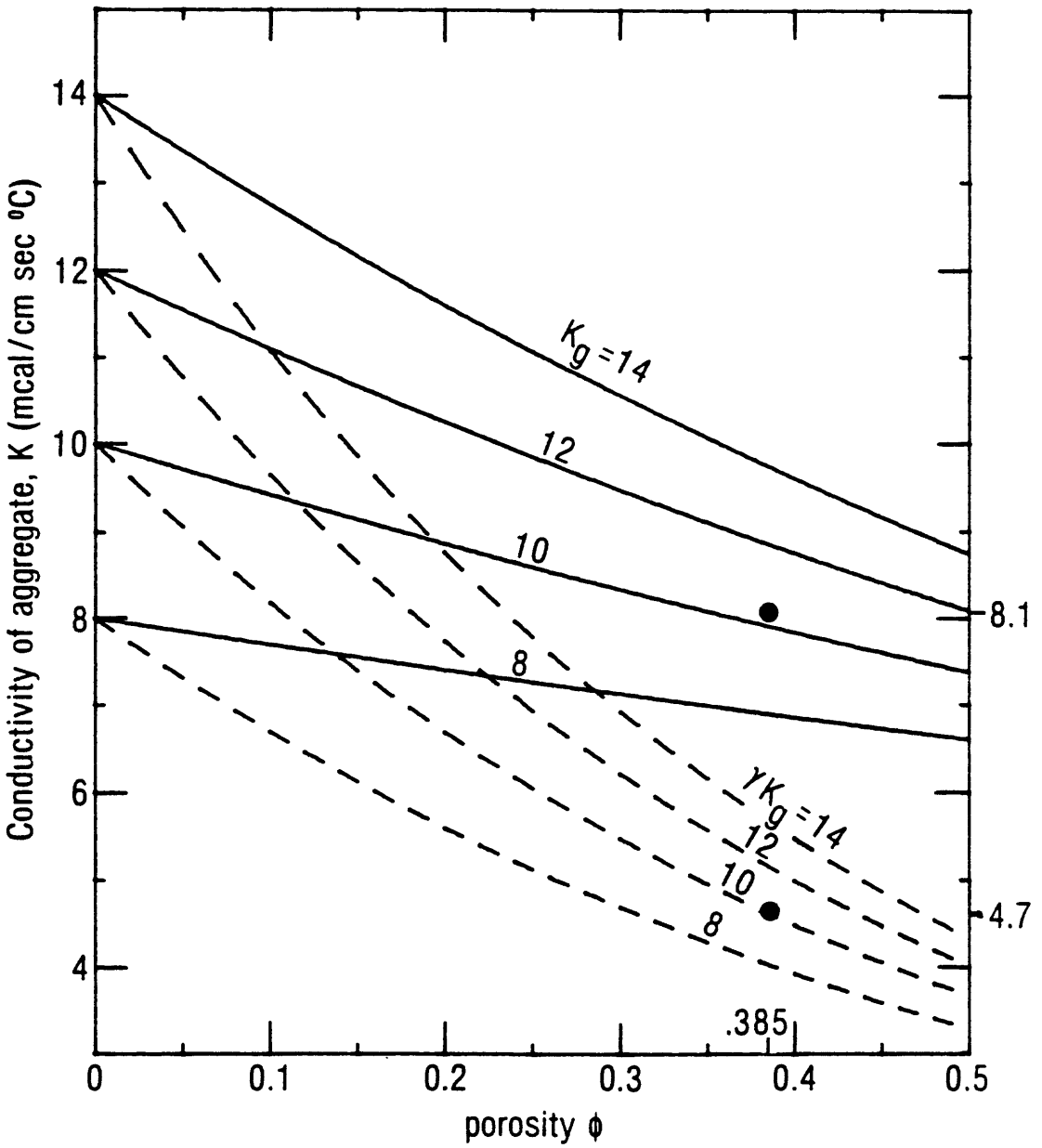
Conductivity of aggregate, K (mcal/cm sec °C)
14
12
10
8
6
4
0
0.1
0.2
0.3
0.4
0.5
porosity ϕ
K_g =14
12
10
8
γK_g =14
12
10
8
8.1
4.7
.385

Figure 7

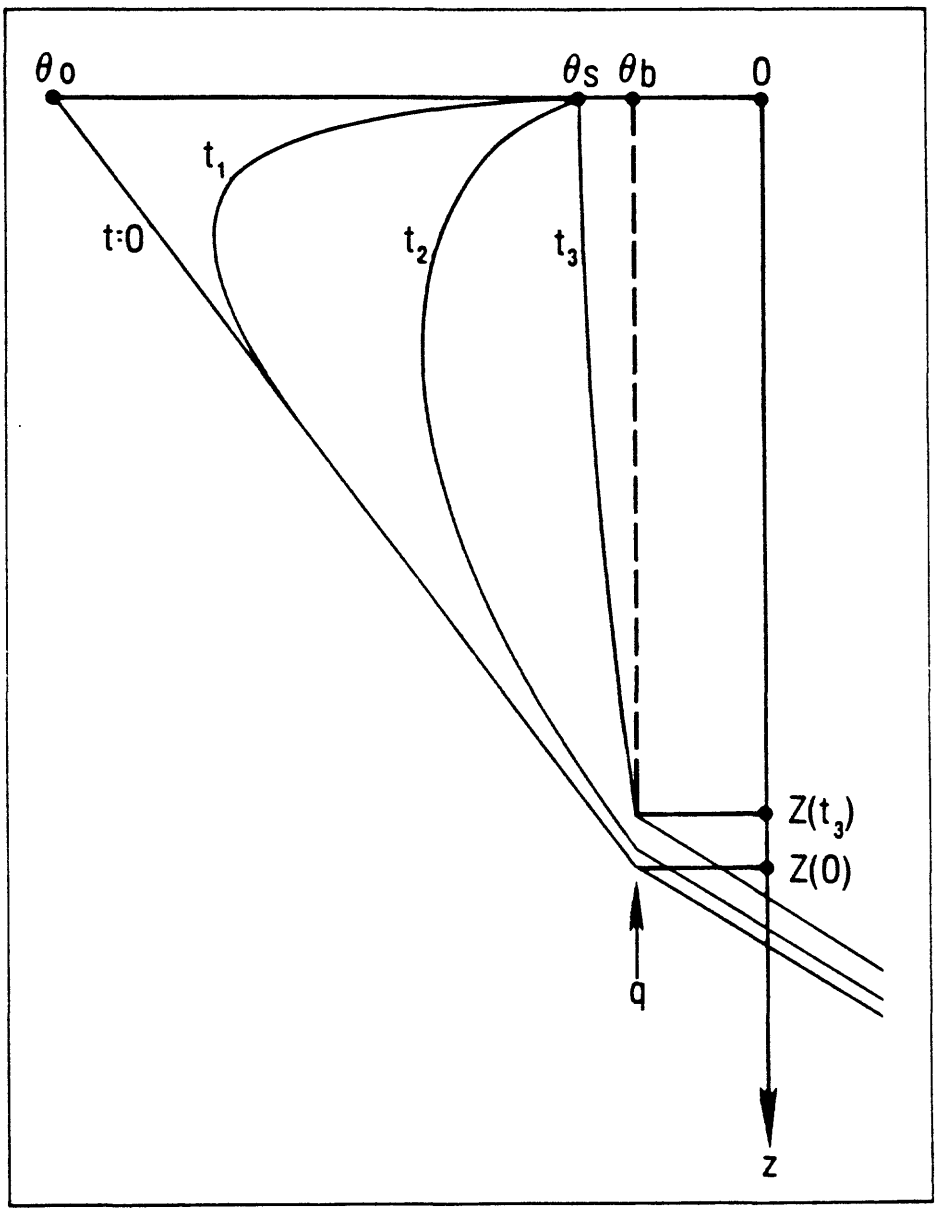

Figure 8

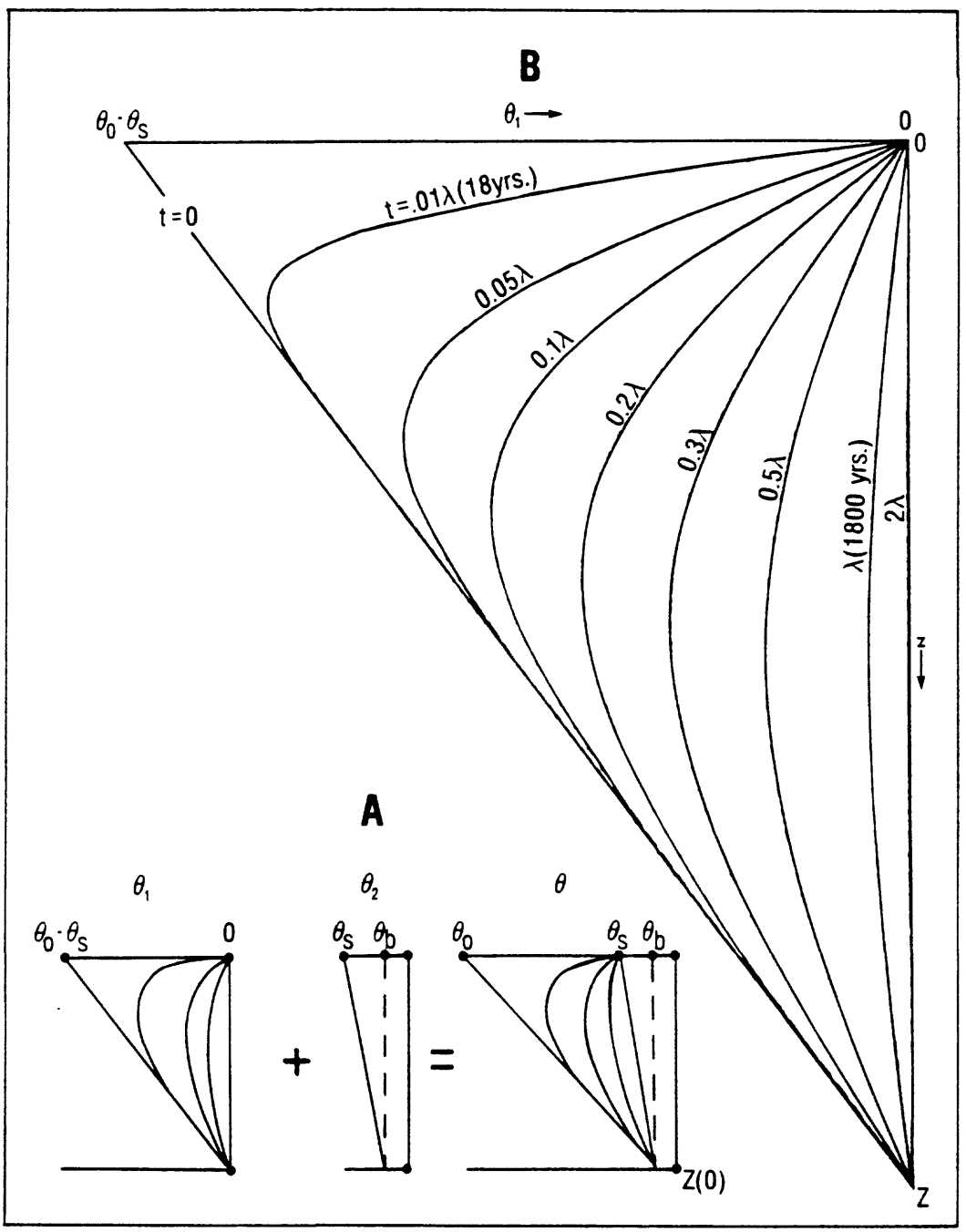
B
$\theta_0 \cdot \theta_S$
θ_1
0
0
t=0
t=.01λ(18yrs.)
0.05λ
0.1λ
0.2λ
0.3λ
0.5λ
λ(1800 yrs.)
2λ
z
A
θ_1
$\theta_0 \cdot \theta_S$
0
θ_2
θ_S θ_D
θ
θ_0
θ_S θ_D
+
=
Z(0)
Z

Figure 9

APPENDIX A. Thermal conductivity of a saturated aggregate

We shall develop a formal relation for the thermal conductivity of a saturated soil in terms of the thermal conductivity of its constituents and the state of its moisture. We start with the assumption that the thermal conductivity, K, of the aggregate can be expressed in terms of the conductivities of its (n) constituents K_1, K_2, K_3 ... K_n and their respective volume fractions ϕ_1, ϕ_2, ϕ_3 ... ϕ_n as follows

$$K = K_1^{\phi_1} K_2^{\phi_2} \ldots K_n^{\phi_n} \qquad \text{(A-1a)}$$

where $$\phi_1 + \phi_2 + \phi_3 + \ldots \phi_n = 1 \qquad \text{(A-1b)}$$

This relation has generally been quite successful when applied to aggregates whose constituent conductivities do not differ by more than one order of magnitude [Woodside and Messmer, 1961], and in particular to saturated earth materials [Sass et al., 1971].

The following notation will be used for volume fractions:

ϕ = volume fraction of water in thawed saturated sample (= porosity).

ϕ_i = volume fraction of ice in frozen sample.

ϕ' = volume fraction of liquid water in frozen sample.

The unfrozen volume fraction ϕ' in the "frozen state" is retained for generality, as it will be important elsewhere in arctic Alaska where fine-grained sediments prevail. It will subsequently be neglected in applications to the coarse sediments near Prudhoe Bay.

In order to account for the variation in conductivity with temperature, we shall define the conductivity symbols in terms of reference temperatures. For conditions in the frozen state we shall use -5°C, and in the thawed state

we shall use +2°C; these values correspond approximately to the mean temperatures of the intervals over which the gradients were determined in the Prudhoe Bay holes. The following notation is used:

K_i = thermal conductivity of ice at -5°C.

K_w = thermal conductivity of water at +2°C.

K_g = geometric mean conductivity of mineral grains at -5°C.

γK_g = geometric mean conductivity of mineral grains at +2°C.

K_{th} = conductivity of thawed soil at +2°C.

K_{fr} = conductivity of frozen soil at -5°C.

The parameter γ adjusts the grain conductivity K_g at the reference temperature of -5°C to the appropriate value γK_g at +2°C. The conductivity of most silicate grains decreases about 0.25% for each °C increase in temperature (Birch and Clark, 1940). Hence the fractional decrease in grain conductivity from the frozen state (-5°C) to the thawed state (+2°C) is

$$\gamma \sim 1 - 0.0025°C^{-1} \times 7°C \qquad \text{(A-3a)}$$

$$= .9825 \qquad \text{(A-3b)}$$

and $\ell n\gamma = -0.0177$ (A-3c)

According to (A-1) the thermal conductivity of the thawed aggregate at the reference temperature of +2°C is given by

$$K_{th} = K_w^{\phi} (\gamma K_g)^{1-\phi} \qquad \text{(A-4)}$$

The conductivity of the "frozen" soil (with volume-fraction ϕ' unfrozen) at -5°C is given by

$$K_{fr} = K_i^{\phi_i} K_w^{\phi'} K_g^{1-(\phi_i+\phi')} \qquad \text{(A-5)}$$

Equations A-4 and A-5 are applied to 2 cases: (1) In the text, to the change in conductivity (in situ) with depth when we pass from frozen to thawed

materials and (2) in Appendix B, to compare the conductivities measured in the laboratory on samples in the frozen and thawed conditions. In each case, it is likely that the relation between the volume-fractions of ice and water is approximately

$$\phi \cong \phi_i + \phi' \qquad \text{(A-6)}$$

i.e., insofar as these applications are concerned, the total porosity is the same in the frozen and thawed state. In an engineering study of the frozen core (unpublished report, BP Alaska, Inc., see Appendix B), it was found that there was no excess ice, but the sediment was saturated. On this basis, the study concludes that the section was frozen from the top downward after deposition, and that the excess water was excluded from the pores as the ice formed within them [see also Howitt, 1971]. For such conditions, it is likely that the porosity would not change across the base of permafrost in an otherwise uniform formation. For the second case (Appendix B), the conductivity was determined with a needle probe in the interior of the sample, initially when the core was saturated with ice, and later when the sample was thawed. We believe the volume loss on thawing was accommodated largely by moisture migration from the edges of the sample, and that the pore space in the interior remained saturated with liquid water.

With the simplification (A-6), we can now express (A-5) by

$$K_{fr} = K_i^{\phi} \; K_g^{1-\phi} \; \left(\frac{K_w}{K_i}\right)^{\phi'} \qquad \text{(A-7)}$$

The last factor in (A-7) contains the effects of unfrozen water on the conductivity of the frozen aggregate. Using the following values from Dorsey [1940]:

$$K_i = 5.45 \frac{\text{mcal}}{\text{cm sec °C}} \text{ at } -5°C \tag{A-8a}$$

$$K_w = 1.34 \frac{\text{mcal}}{\text{cm sec °C}} \text{ at } +2°C \tag{A-8b}$$

we obtain representative values for that factor:

$$\left(\frac{K_w}{K_i}\right)^{\phi'} \cong 0.99, \quad \phi' = 1\% \tag{A-9a}$$

$$\cong 0.90, \quad \phi' = 7\tfrac{1}{2}\% \tag{A-9b}$$

For the coarse-grained sediments under study, we generally expect

$$\phi' \lesssim 1\% \tag{A-10}$$

in which case

$$K_{fr} \cong K_i^{\phi} K_g^{1-\phi} \tag{A-11}$$

Combination of A-4 and A-11 now yields an expression for the porosity ϕ in terms of conductivities as follows:

$$\phi = \frac{\ell n \frac{K_{fr}}{K_{th}} + \ell n\gamma}{\ell n \frac{K_i}{K_w} + \ell n\gamma} \tag{A-12a}$$

$$= 0.722 \left(\ell n \frac{K_{fr}}{K_{th}} - 0.013\right) \tag{A-12b}$$

The numerical values used in A-12b are from A-3 and A-8.

APPENDIX B. Direct measurements on frozen cores

The analysis in the text, which leads to estimates of porosity, ice content, thermal conductivity, and finally heat flow is based upon physical models and assumptions, which at each step, might be suspected of introducing considerable uncertainty. To test these procedures, we made direct measurements on samples of frozen core from a test well in the Prudhoe Bay field (BP12-10-14, located by the star in Figure 1). Although much of the 600-m permafrost section was cored, we tested only six samples (Table B-1) representing three meters or so of material between the depths of 200 and 330 m. The samples were kindly made available to us by BP Alaska, Inc., under whose auspices the entire core collection was studied thoroughly to determine engineering properties ('Coring and Testing Permafrost to a Depth of 1858 feet,' a report prepared for BP Alaska, Inc., by Adams, Corthell, Lee, Wince, and Associates, unpublished, 1970). Their studies revealed that the sediments were coarse grained and that the pore spaces were generally completely filled with ice, but the mineral grains were generally in mutual contact. These observations support the assumption that the ice content by volume is approximately equal to the porosity. The studies also revealed that the porosity was high, generally about 40%. This is consistent with the porosities calculated for the nine holes summarized in Table 2, and it supports the assumptions made in those calculations, i.e., that the observed thermal gradient contrast represents a steady-state in materials that are homogeneous except for the state of their water, and that the geometric mean theory for conductivity applies to these materials (equations (10) and (11); see also Appendix A).

For further confirmation, we measured the thermal conductivity of the frozen cores in our laboratory and then thawed them and repeated the measurements. Results from these measurements on the six samples (adjusted to the reference temperatures of -5°C and +2°C) are summarized in columns 8 and 11 of Table B-1. For comparison with those directly measured values, we calculated conductivities as we did for the nine boreholes by using equations (10) and (11). For this calculation, ϕ was obtained from direct measurements made on contiguous core pieces in the engineering study (ϕ_m, Table B-1) and grain conductivity (K_g, Table B-1) was measured for each core in the laboratory as before. Comparison of the grain conductivities K_g in Table B-1 (which average 14.01 cal/cm sec °C) with those in Table 2 (which average 10.24 cal/cm sec °C) suggests that our small sample of the cored section was biased toward the more siliceous and hence more conductive, materials. The last two columns of Table B-1 show remarkably good agreement between the directly measured conductivities of the thawed materials (averaging 5.34 cal/cm sec °C) and the corresponding values calculated from equation (11) (averaging 5.35 mcal/cm sec °C). For the frozen samples, the agreement is less satisfactory; the values calculated by equation (10) average 9.51 mcal/cm sec °C, which is 12% greater than the average (8.51 mcal/cm sec °C) of the directly measured values. The discrepancy probably results from the formation of micro-cracks during decompression of the brittle frozen core from its natural state. Walsh and Decker [1966] have shown that such dry micro-cracks in crystalline rocks typically reduce the conductivity by this amount.

We believe that these experiments on core samples provide a basis for confidence in the estimates of in situ conductivity (frozen and thawed), heat flow, porosity, and ice content summarized for the upper 750 m section at Prudhoe Bay in Table 2.

TABLE B-1. Measurements on core samples from hole 12-10-14

(1)	(2)	(3)	(4)	(5)	(6)	(7)	(8)	(9)	(10)	(11)	(12)
Depth interval (m)		Material	Porosity	K_g (-5°C)		K_{fr} (-5°C)			K_{th} (+2°C)		
From	To		ϕ_m	N	Measured value	N	Measured value	Calculated value	N	Measured value	Calculated value
199.5	199.9	SP	.431	3	13.82	7	8.11	9.25	3	4.89	5.01
244.1	245.0	ML	.402	3	14.15	6	8.73	9.64	5	5.10	5.43
309.6	310.1	SP	.405	6	13.46	8	8.76	9.33	7	5.75	5.23
351.3	351.6	SP	.387	3	13.97	9	8.31	9.70	9	5.42	5.58
432.2	432.8	SP	.389	0	(14.0)	6	8.48	9.45	6	5.61	5.52
331.0	331.7	SP	.418	1	14.67	6	8.69	9.70	6	5.27	5.34
Mean			.405	5	14.01	6	8.51	9.51	6	5.34	5.35
(±Std. Dev.)			(±.017)		(±.45)		(±.26)	(±.20)		(±.32)	(±.21)

Column (3) SP, poorly graded clean sand; ML, dense silt.

Column (4) Porosity ϕ_m measured on a contiguous frozen sample.

Columns (8) and (11) Mean of N measured values adjusted to the temperature indicated (-5°C or +2°C).

Columns (9) and (12) Calculated from measured values of porosity ϕ_m and grain conductivity K_g (using equation 10 or 11).

APPENDIX C

Temperature observations in the 14 wells listed in Table 1 are presented graphically in Figures C-1 through C-14 in the format of Figure 4 of the text. The measurements were made at discrete depths (usually at intervals of 5-10 m) with a multiconductor cable and thermistor thermometer using the "portable mode" described by Sass et al. [1971]. Although the intrinsic sensitivity of the system for differential temperature measurements is better than one millidegree, most of the observations were made under adverse field conditions, the effects of which are difficult to assess. Judging from repeated observations in the same hole using different thermometers, the error in absolute temperature is probably less than 0.1°C in general although errors of a few tenths are obvious in some of the profiles (see e.g., the ragged portion of the curve below 700 m for τ = 26.8 in PBA, Figure C-1, and the portion below 460 m on the curve τ = 18 in PBE, Figure C-5).

Inasmuch as the drilling disturbance resulted in a positive heat source at the depths studied, we generally expect observations in the same hole to indicate lower temperatures with each successive reading at each depth. However, this is not always the case; some of the exceptions can be attributed to the error in absolute temperature and others cannot. For example in PBE, Figure C-5, above 150 m the temperatures at τ = 18 are up to 0.1°C higher than those at the earlier time τ = 15.6. We believe this represents error in the measurements of temperature and/or depth in some combination. Note also that in PBF, Figure C-6, the portion of curve τ = 0.11 below 600 m is warmer than the two subsequent profiles (τ = 0.3 and 0.5) in the same depth range. For this profile the measurements were widely spaced (~30 m) and the discrepancy could be the result of gross observational error at only one or possibly two

points; we cannot, however, be certain that is the cause. In Figure 4 of the text we deleted this portion of the curve for simplicity, as it was not needed for the analysis of equilibrium temperatures.

Unlike in the above examples, the increase in temperature with time near the base of permafrost (550-600 m, curve τ = 13.6) in PBG (Figure C-7) is not likely to be the result of instrumental error. One explanation is that the freezing point was depressed in this region by a build-up of pressure associated with freezing below 600 m and above 550 m (see curve τ = 6.5). Between the reading at τ = 6.5 and τ = 13.6, this pressure was released, possibly by casing collapse or hydraulic fracture, and the intervening 50-m interval froze adiabatically, with the latent heat warming it to the low-pressure freezing temperature. The reversal in hole PBE (Figure C-5) below 540 m for curve τ = 5.1 is more puzzling, and it is difficult to analyze without engineering information. Perhaps it represents downward advection in the borehole caused by a similar pressure build-up, and possibly casing collapse, with return flow in the annulus.

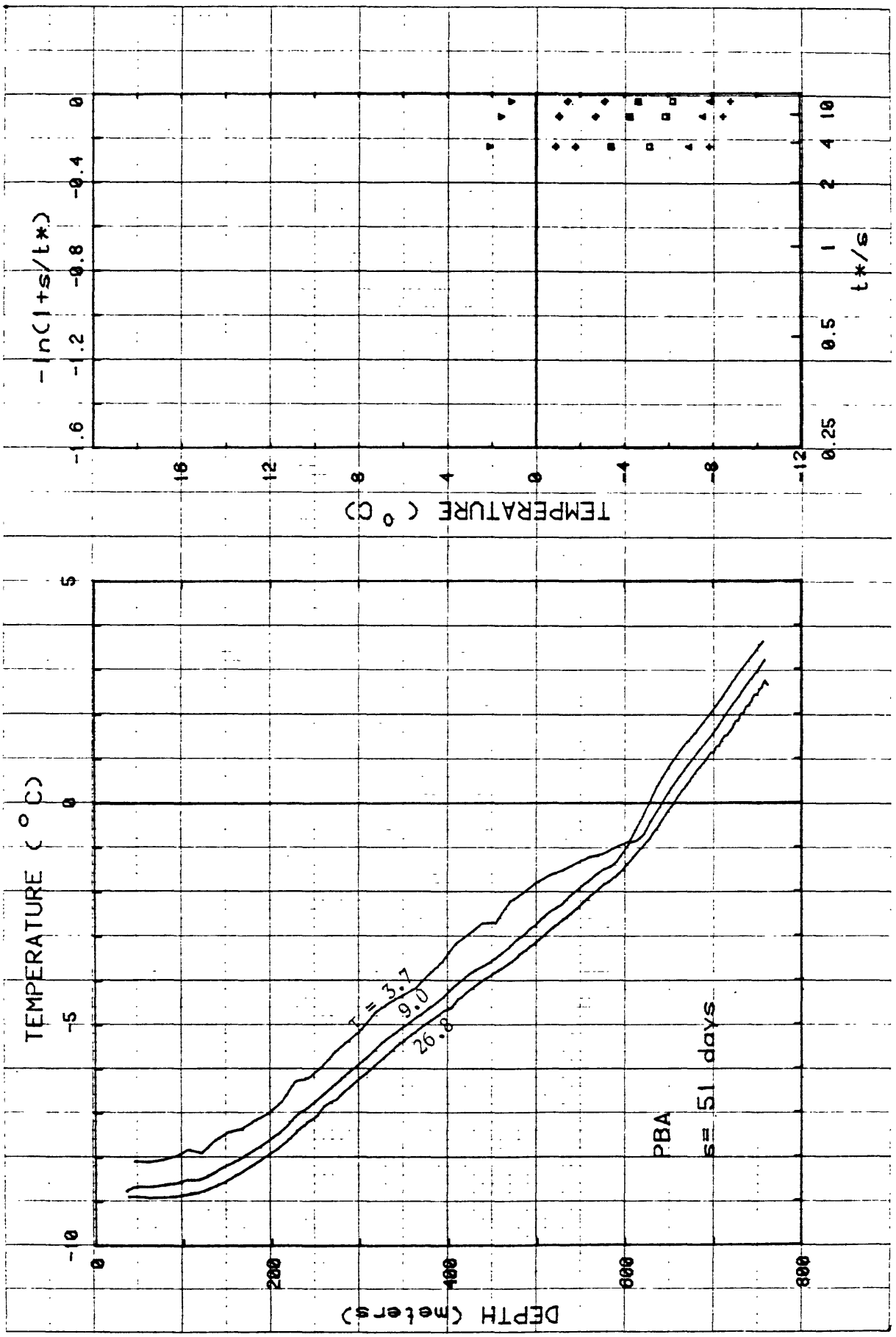
TEMPERATURE (°C)
DEPTH (meters)
PBA
s= 51 days
T = 3.7
9.0
26.8
- ln(1+s/t*)
t*/s
TEMPERATURE (°C)

Figure C-1.

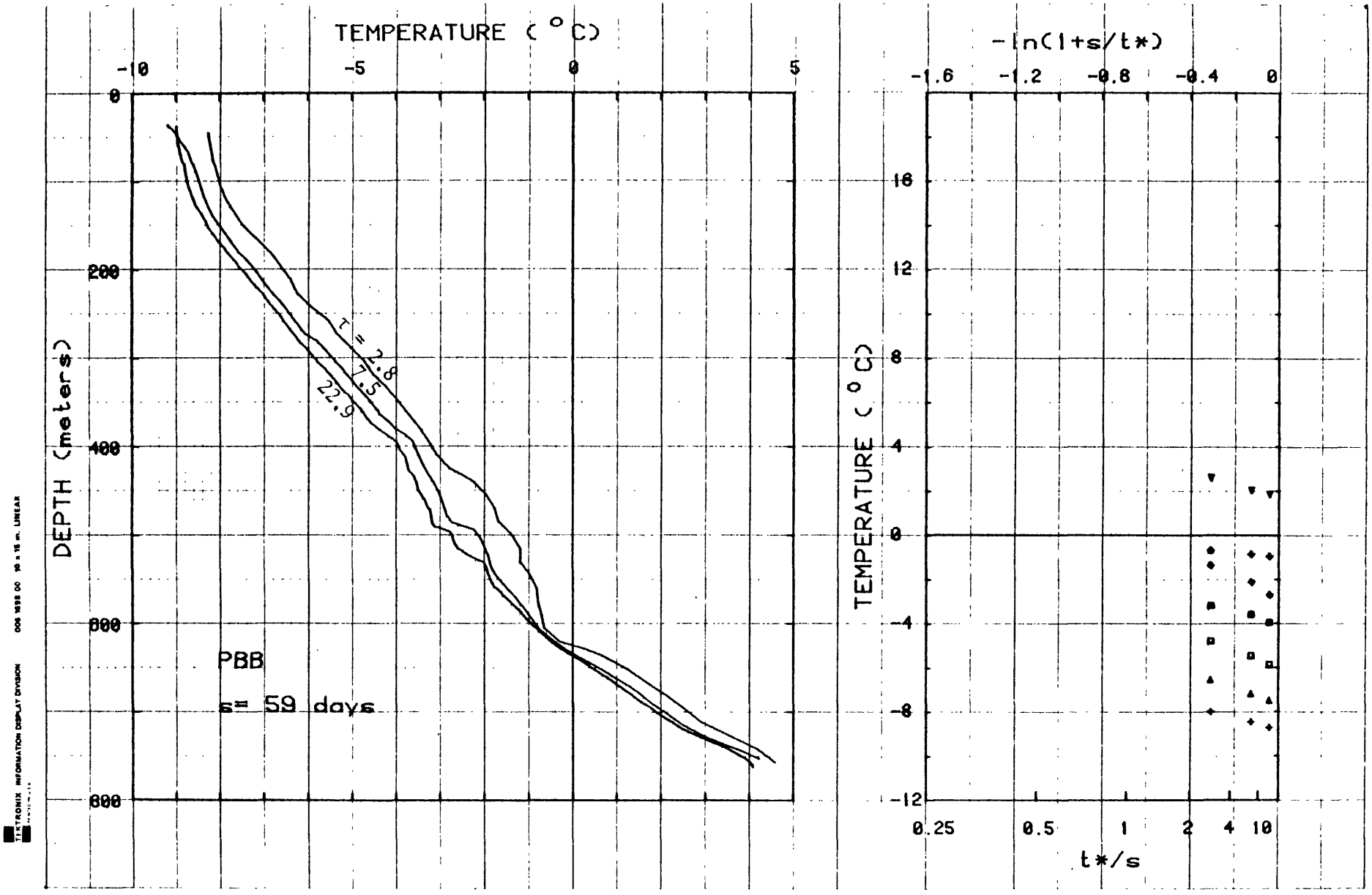
TEMPERATURE (°C)
-10
-5
0
5
0
200
400
600
800
DEPTH (meters)
τ = 2.8
7.5
22.9
PBB
s= 59 days
-ln(1+s/t*)
-1.6
-1.2
-0.8
-0.4
0
16
12
8
4
0
-4
-8
-12
TEMPERATURE (°C)
0.25
0.5
1
2
4
10
t*/s

Figure C-2

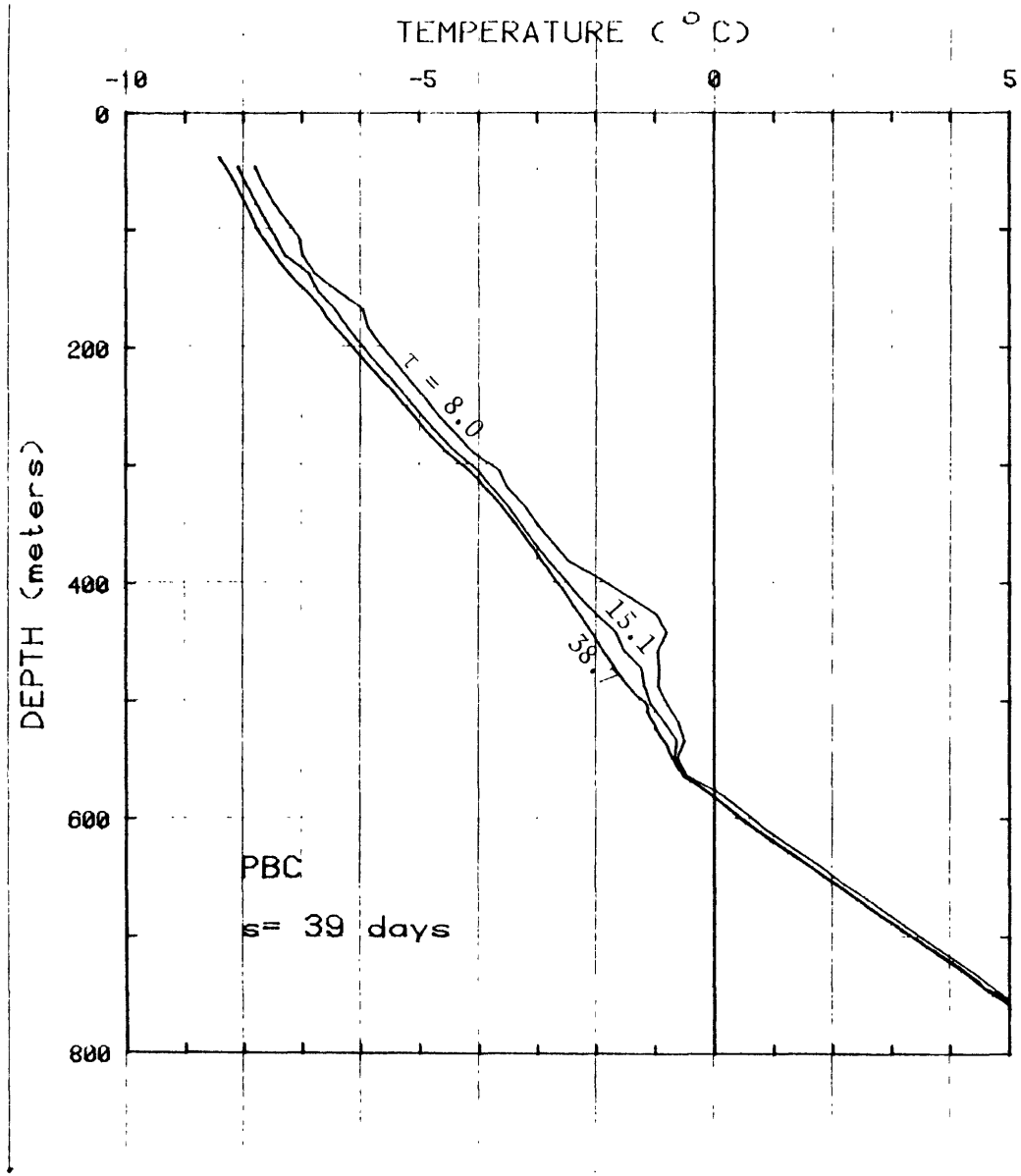
TEMPERATURE (°C)
-10
-5
0
5
0
200
400
600
800
DEPTH (meters)
T = 8.0
15.1
38.1
PBC
s= 39 days

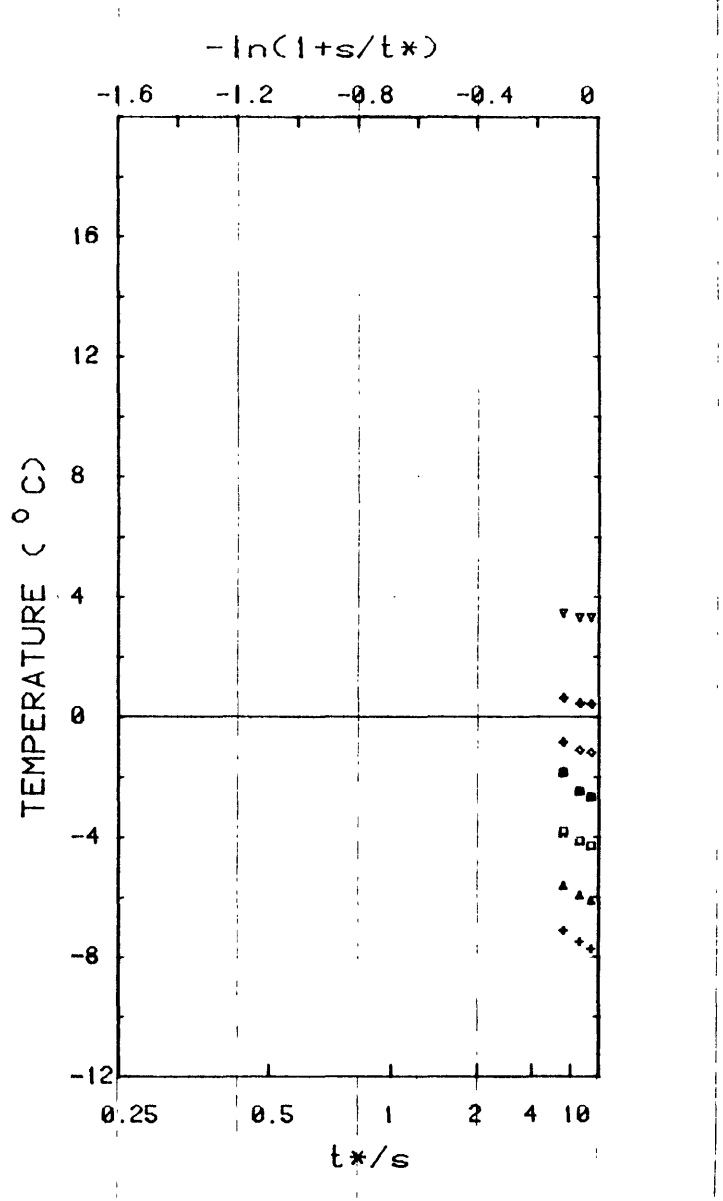
-ln(1+s/t*)
-1.6
-1.2
-0.8
-0.4
0
16
12
8
4
0
-4
-8
-12
TEMPERATURE (°C)
0.25
0.5
1
2
4
10
t*/s

Figure C-3.

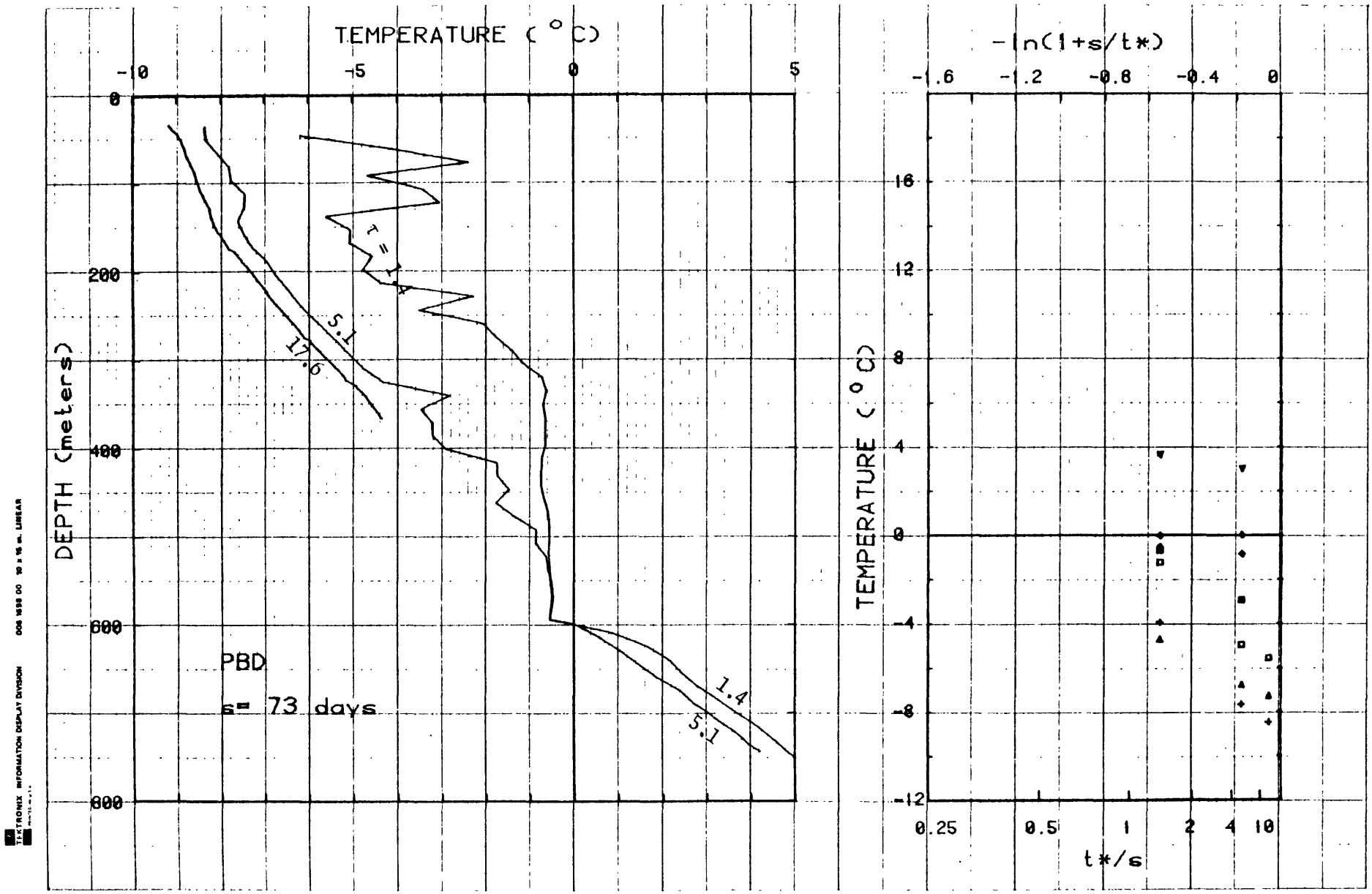
TEMPERATURE (°C)
-10
-5
0
5
DEPTH (meters)
0
200
400
600
800
τ = 1.4
5.1
17.6
PBD
s= 73 days
1.4
5.1
-ln(1+s/t*)
-1.6
-1.2
-0.8
-0.4
0
TEMPERATURE (°C)
16
12
8
4
0
-4
-8
-12
0.25
0.5
1
2
4
10
t*/s

Figure C-4.

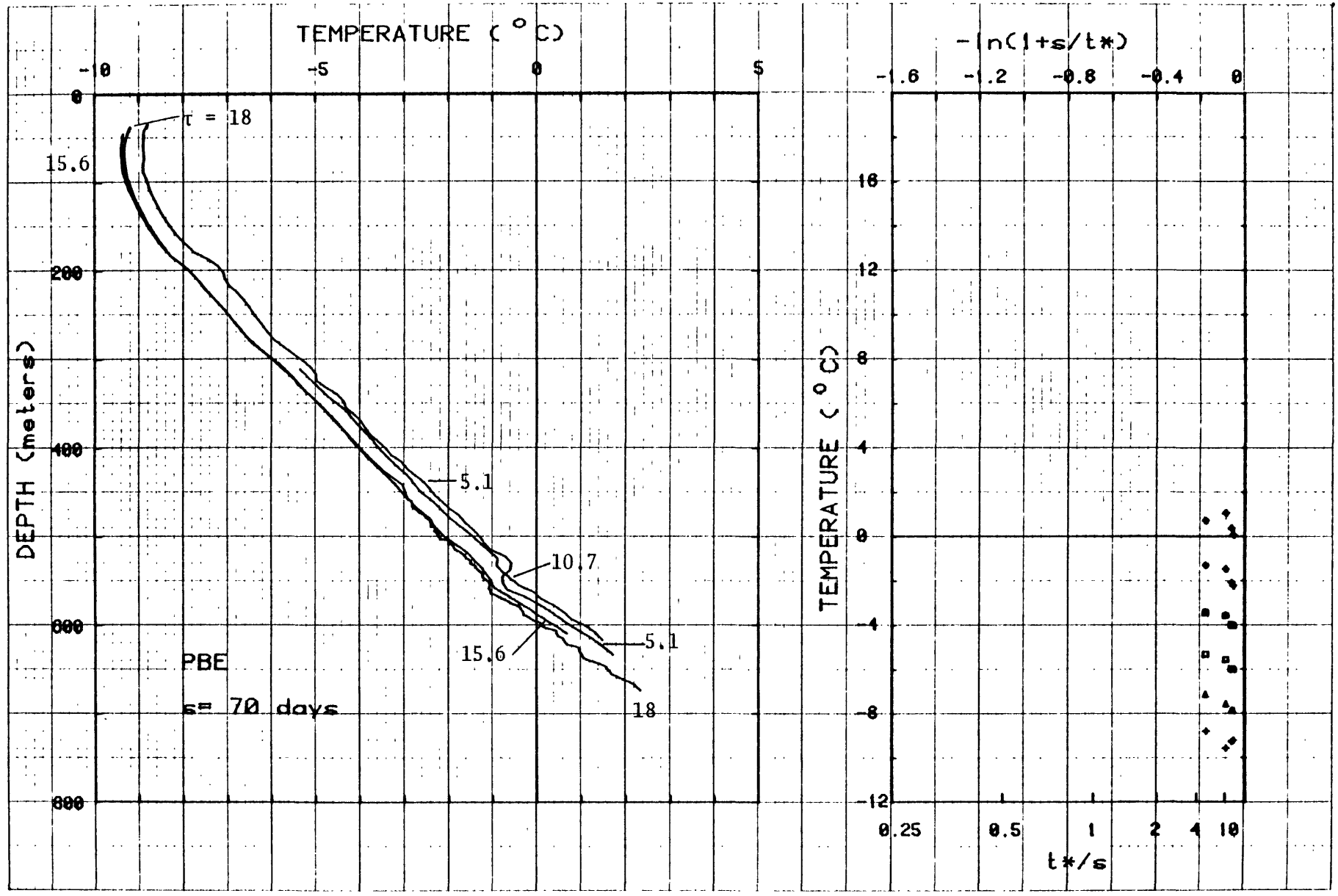
TEMPERATURE (°C)
-10
-5
0
5
DEPTH (meters)
0
200
400
600
800
τ = 18
15.6
5.1
10.7
5.1
15.6
18
PBE
s= 70 days
-ln(1+s/t*)
-1.6
-1.2
-0.8
-0.4
0
TEMPERATURE (°C)
16
12
8
4
0
-4
-8
-12
0.25
0.5
1
2
4
10
t*/s

Figure C-5.

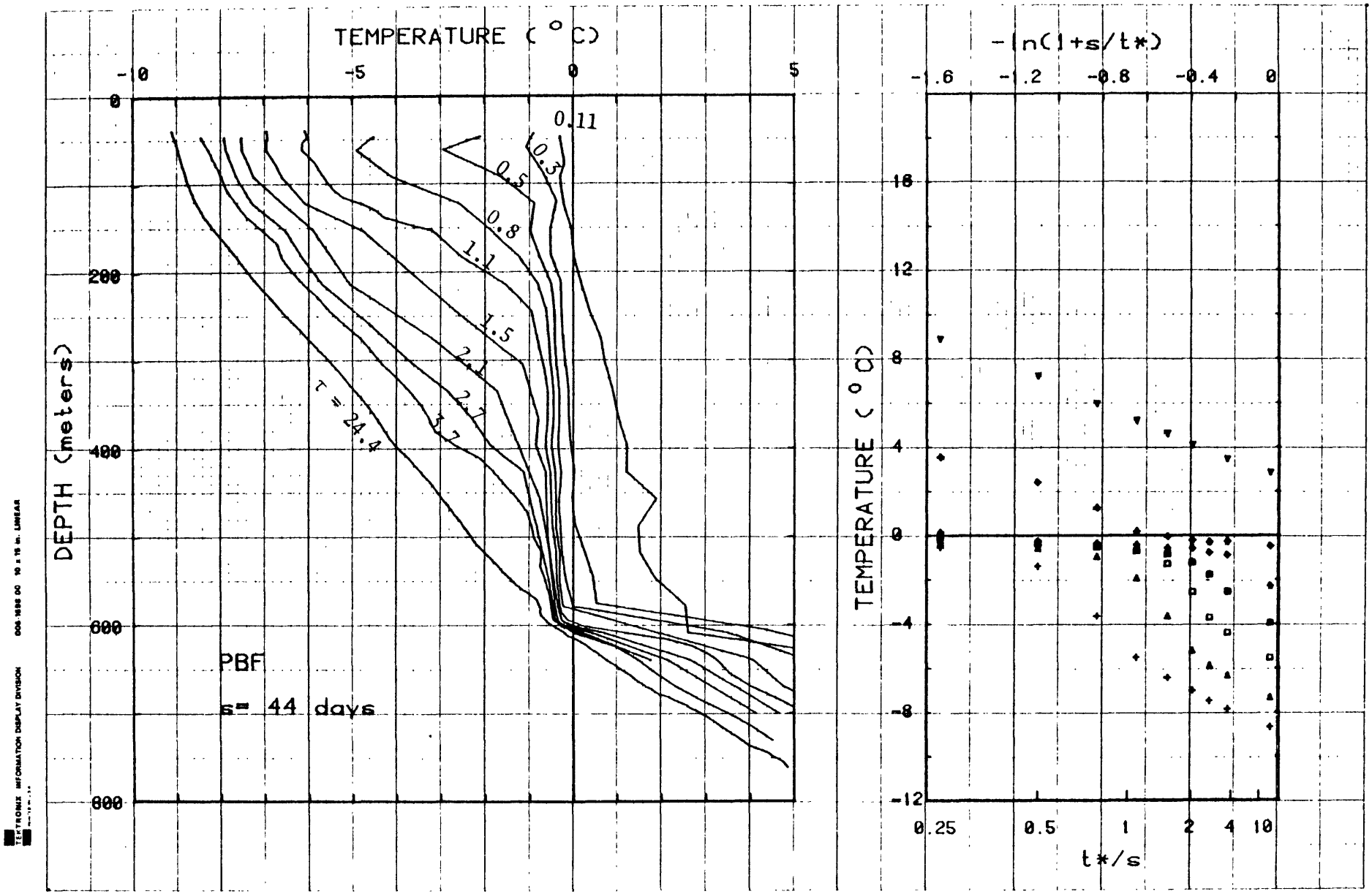
TEMPERATURE (°C)
-10
-5
0
5
0
200
400
600
800
DEPTH (meters)
0.11
0.3
0.5
0.8
1.1
1.5
2.1
2.7
3.7
τ = 24.4
PBF
s= 44 days
-ln(1+s/t*)
-1.6
-1.2
-0.8
-0.4
0
16
12
8
4
0
-4
-8
-12
TEMPERATURE (°C)
0.25
0.5
1
2
4
10
t*/s

Figure C-6.

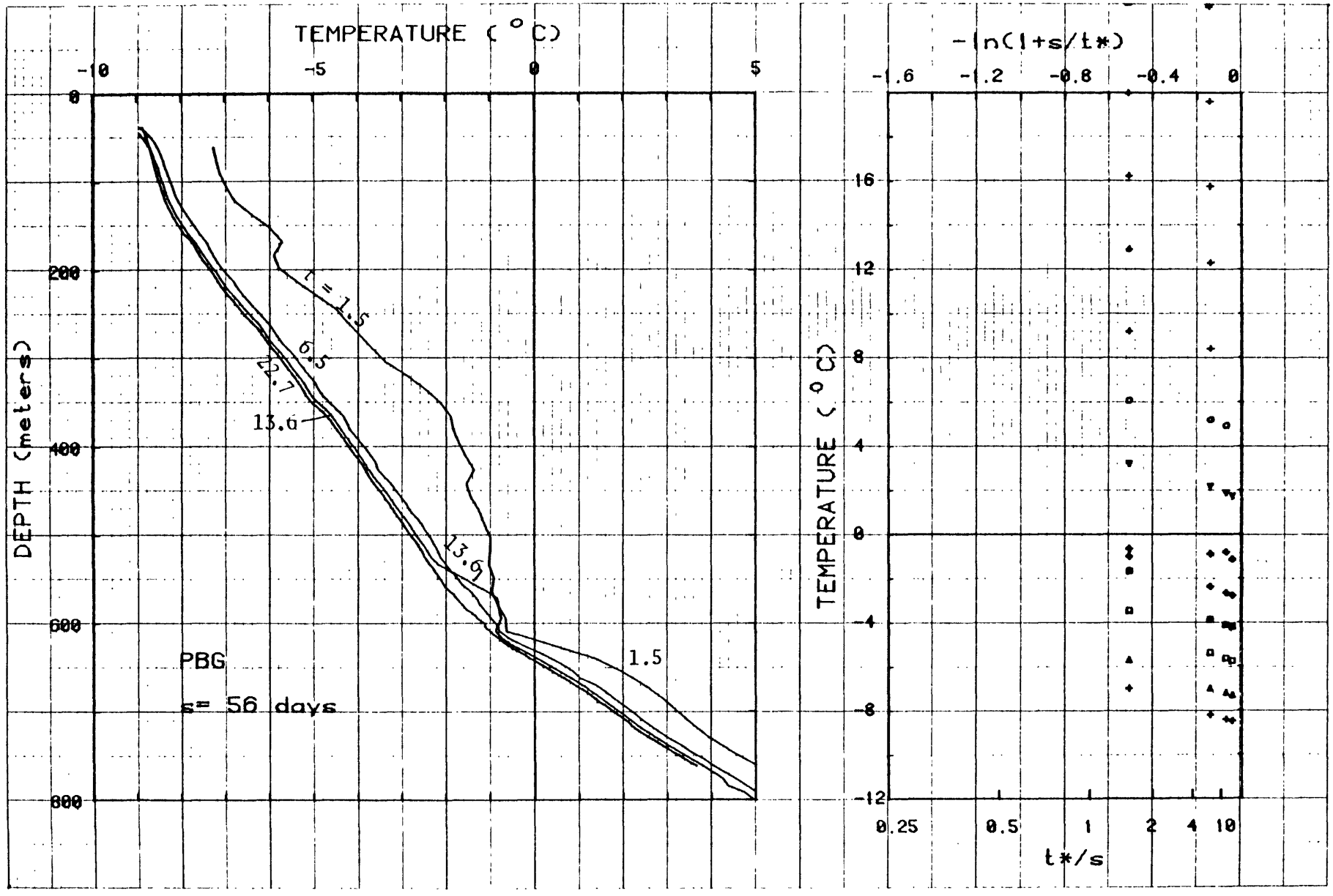
TEMPERATURE (°C)
-10
-5
0
5
DEPTH (meters)
0
200
400
600
800
τ = 1.5
6.5
27.7
13.6
13.6
1.5
PBG
s= 56 days
-ln(1+s/t*)
-1.6
-1.2
-0.8
-0.4
0
16
12
8
4
0
-4
-8
-12
TEMPERATURE (°C)
0.25
0.5
1
2
4
10
t*/s

Figure C-7.

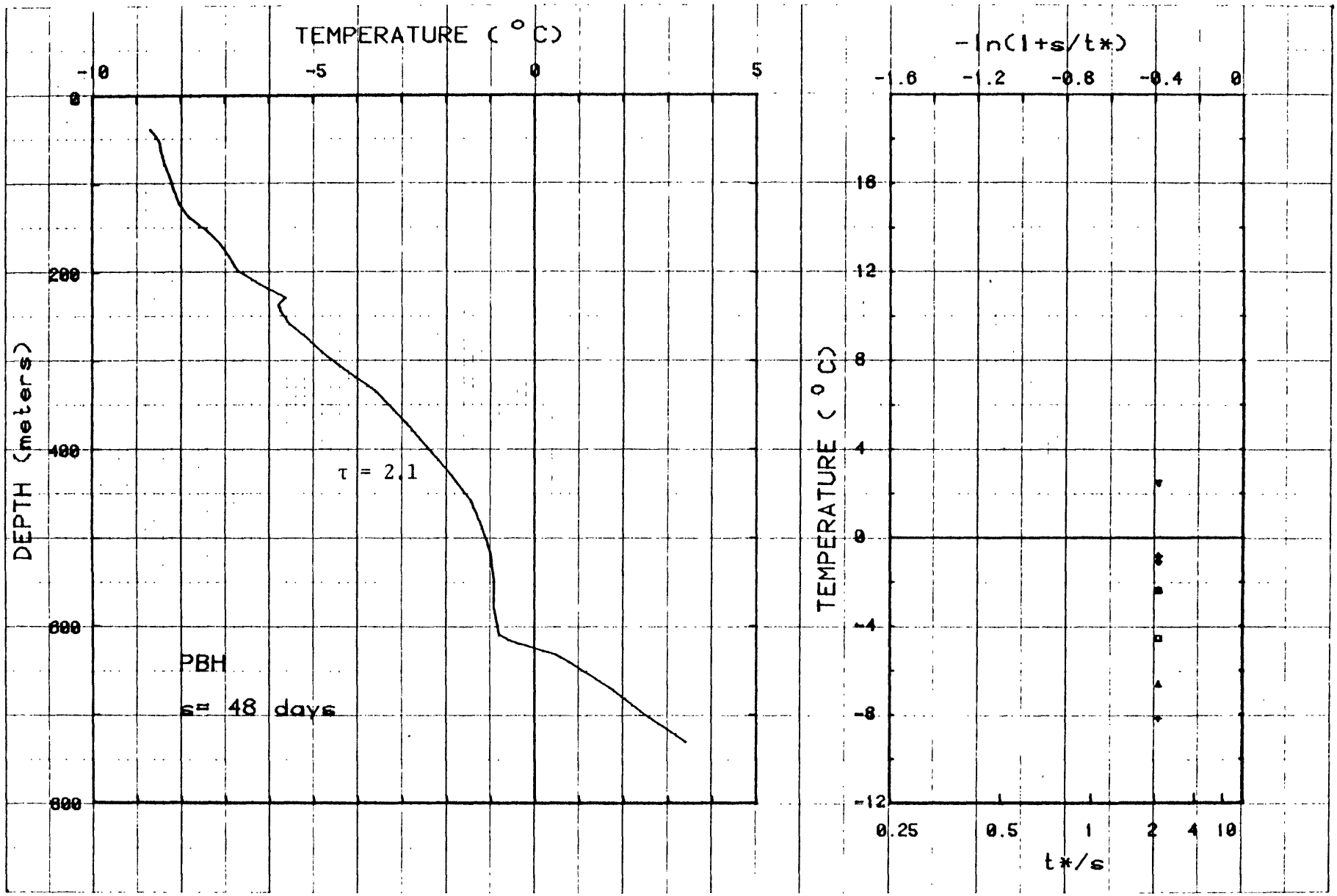
TEMPERATURE (°C)
-10
-5
0
5
0
200
400
600
800
DEPTH (meters)
τ = 2.1
PBH
s= 48 days
-ln(1+s/t*)
-1.6
-1.2
-0.8
-0.4
0
16
12
8
4
0
-4
-8
-12
TEMPERATURE (°C)
0.25
0.5
1
2
4
10
t*/s

Figure C-8.

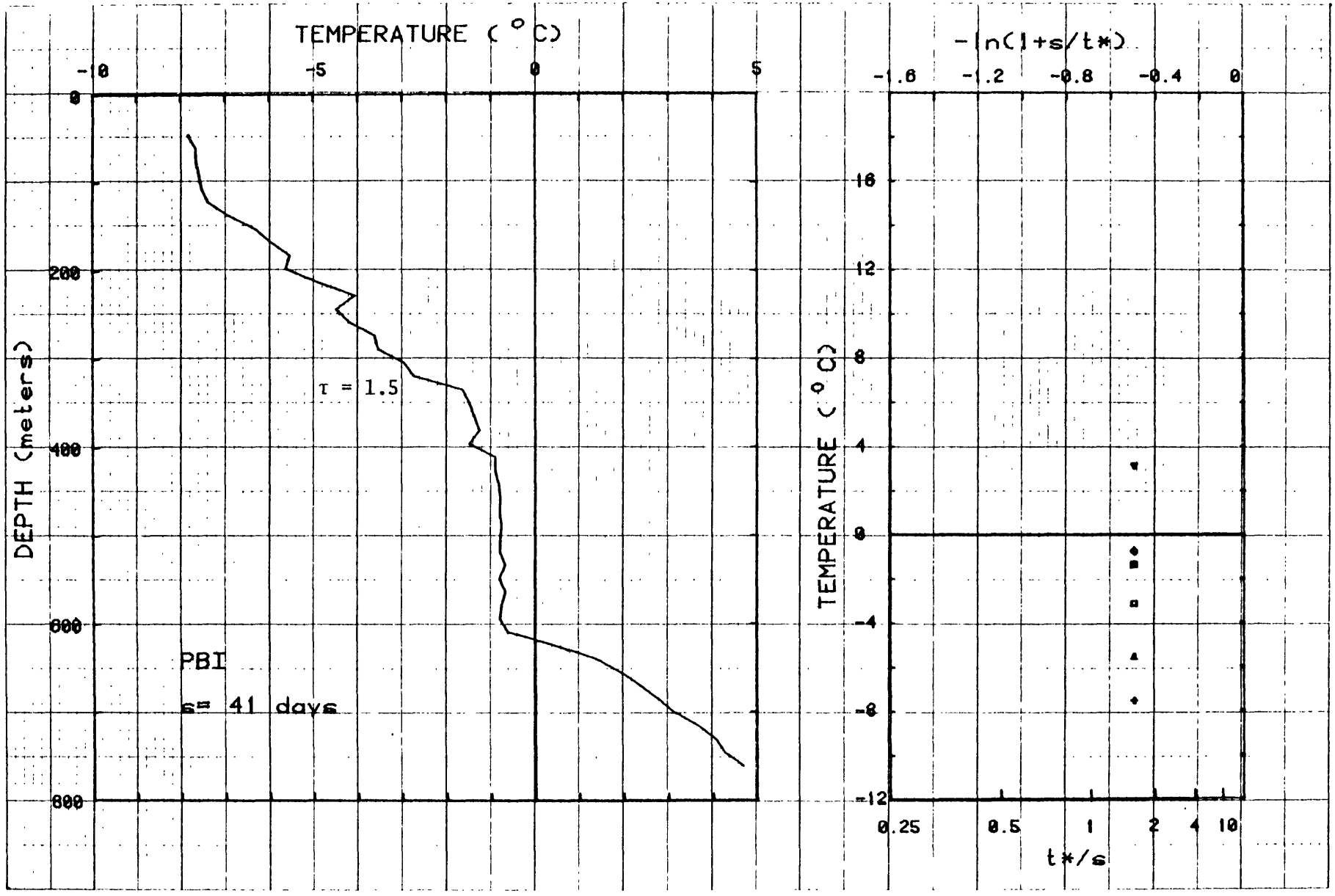
TEMPERATURE (°C)
-10
-5
0
5
DEPTH (meters)
0
200
400
600
800
τ = 1.5
PBI
s= 41 days
-ln(1+s/t*)
-1.6
-1.2
-0.8
-0.4
0
TEMPERATURE (°C)
16
12
8
4
0
-4
-8
-12
0.25
0.5
1
2
4
10
t*/s

Figure C-9.

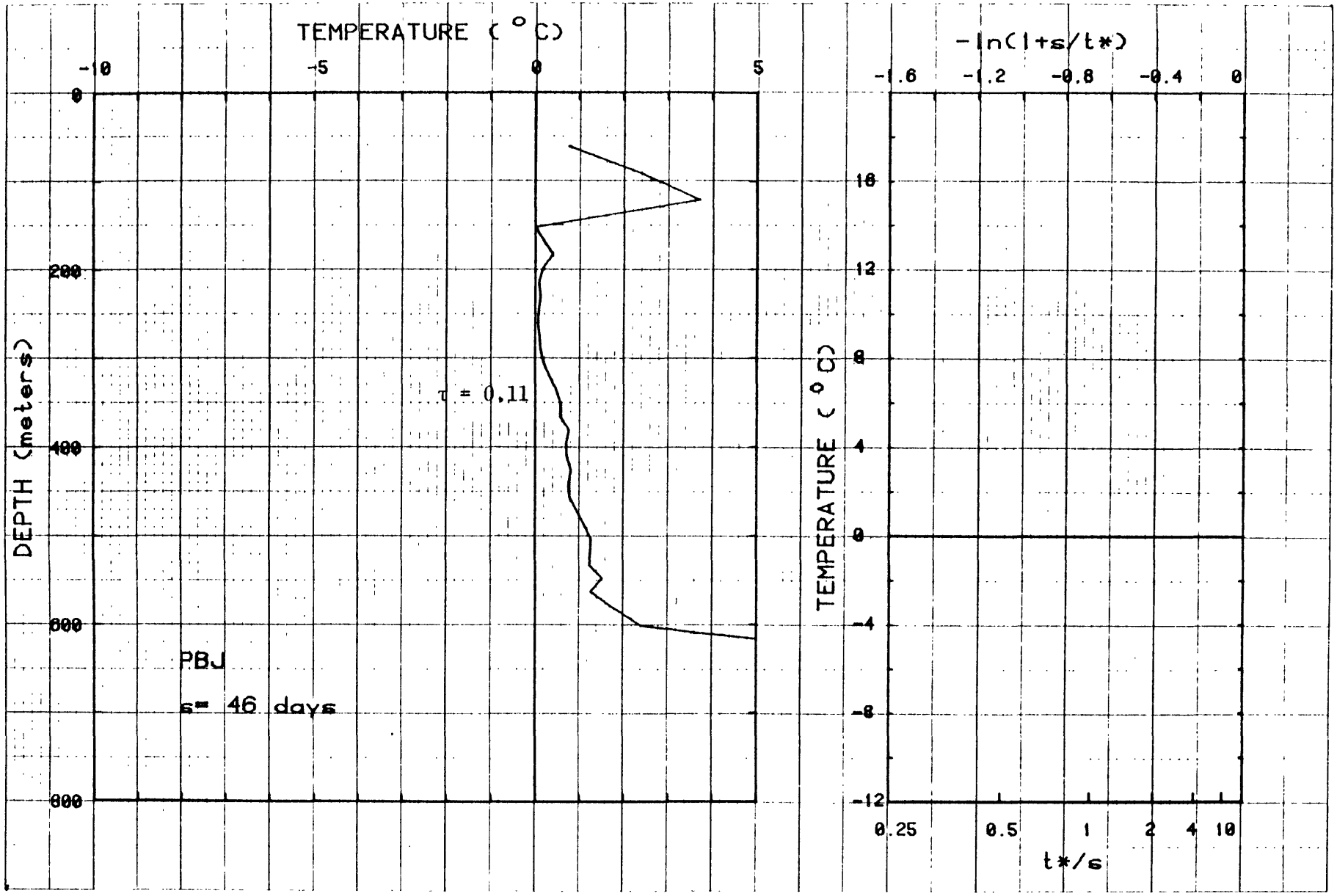
TEMPERATURE (°C)
-10
-5
0
5
DEPTH (meters)
0
200
400
600
800
τ = 0.11
PBJ
s= 46 days
-ln(1+s/t*)
-1.6
-1.2
-0.8
-0.4
0
TEMPERATURE (°C)
16
12
8
4
0
-4
-8
-12
0.25
0.5
1
2
4
10
t*/s

Figure C-10.

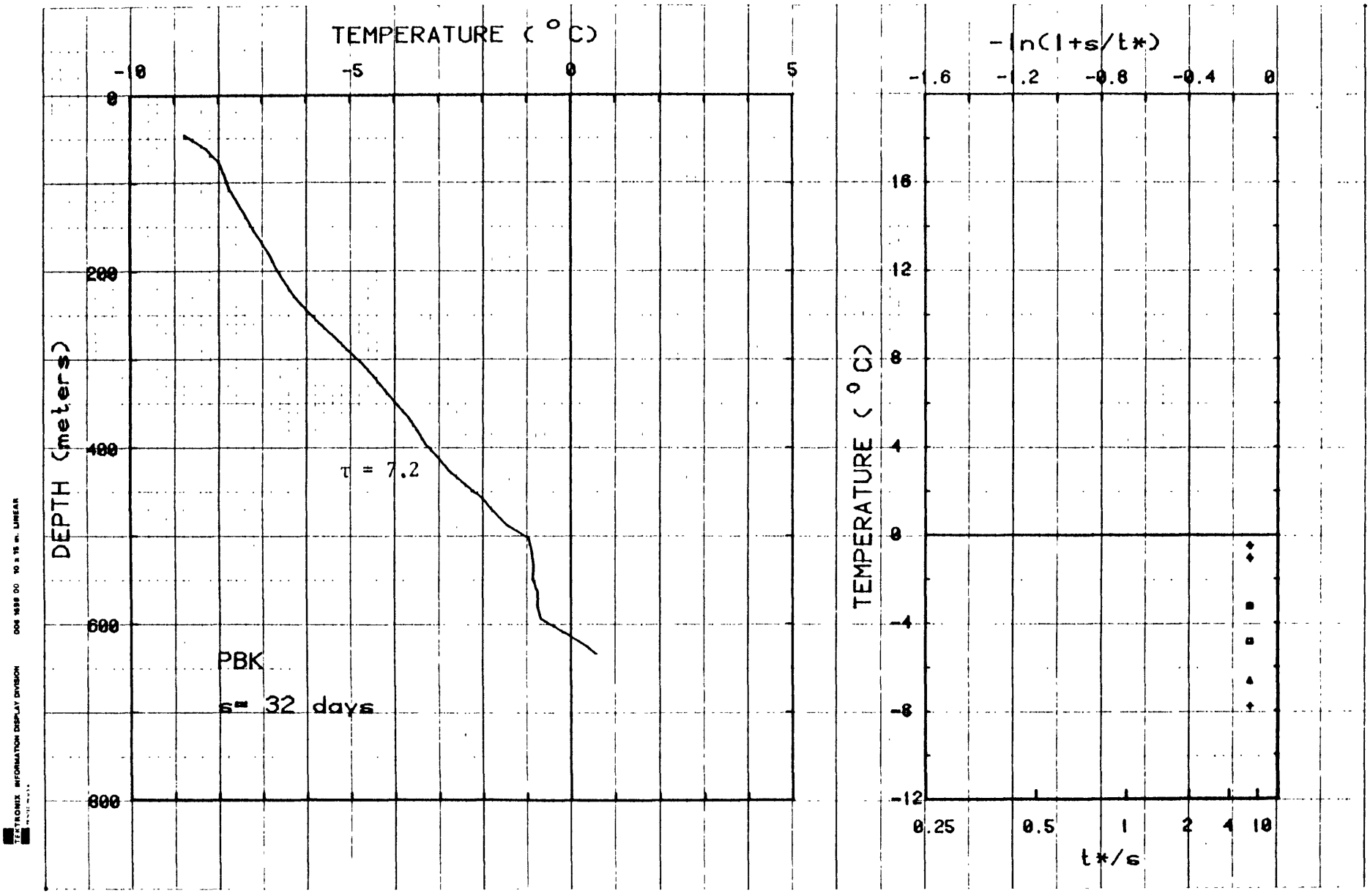
TEMPERATURE (°C)
-10
-5
0
5
DEPTH (meters)
0
200
400
600
800
τ = 7.2
PBK
s= 32 days
-(ln(1+s/t*)
-1.6
-1.2
-0.8
-0.4
0
TEMPERATURE (°C)
16
12
8
4
0
-4
-8
-12
0.25
0.5
1
2
4
10
t*/s
TEKTRONIX INFORMATION DISPLAY DIVISION

Figure C-11.

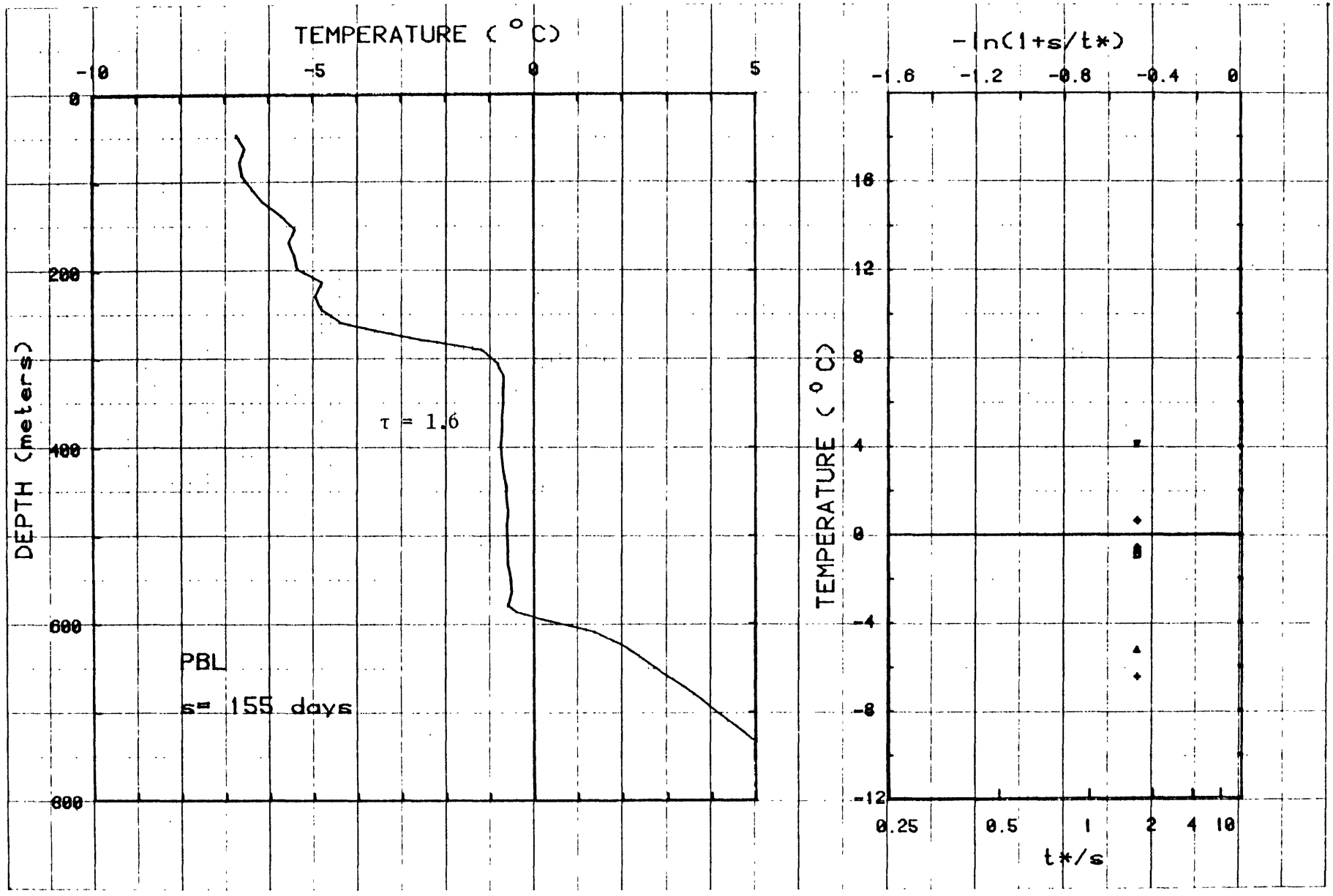
TEMPERATURE (°C)
-10
-5
0
5
0
200
400
600
800
DEPTH (meters)
τ = 1.6
PBL
s= 155 days
-ln(1+s/t*)
-1.6
-1.2
-0.8
-0.4
0
16
12
8
4
0
-4
-8
-12
TEMPERATURE (°C)
0.25
0.5
1
2
4
10
t*/s

Figure C-12.

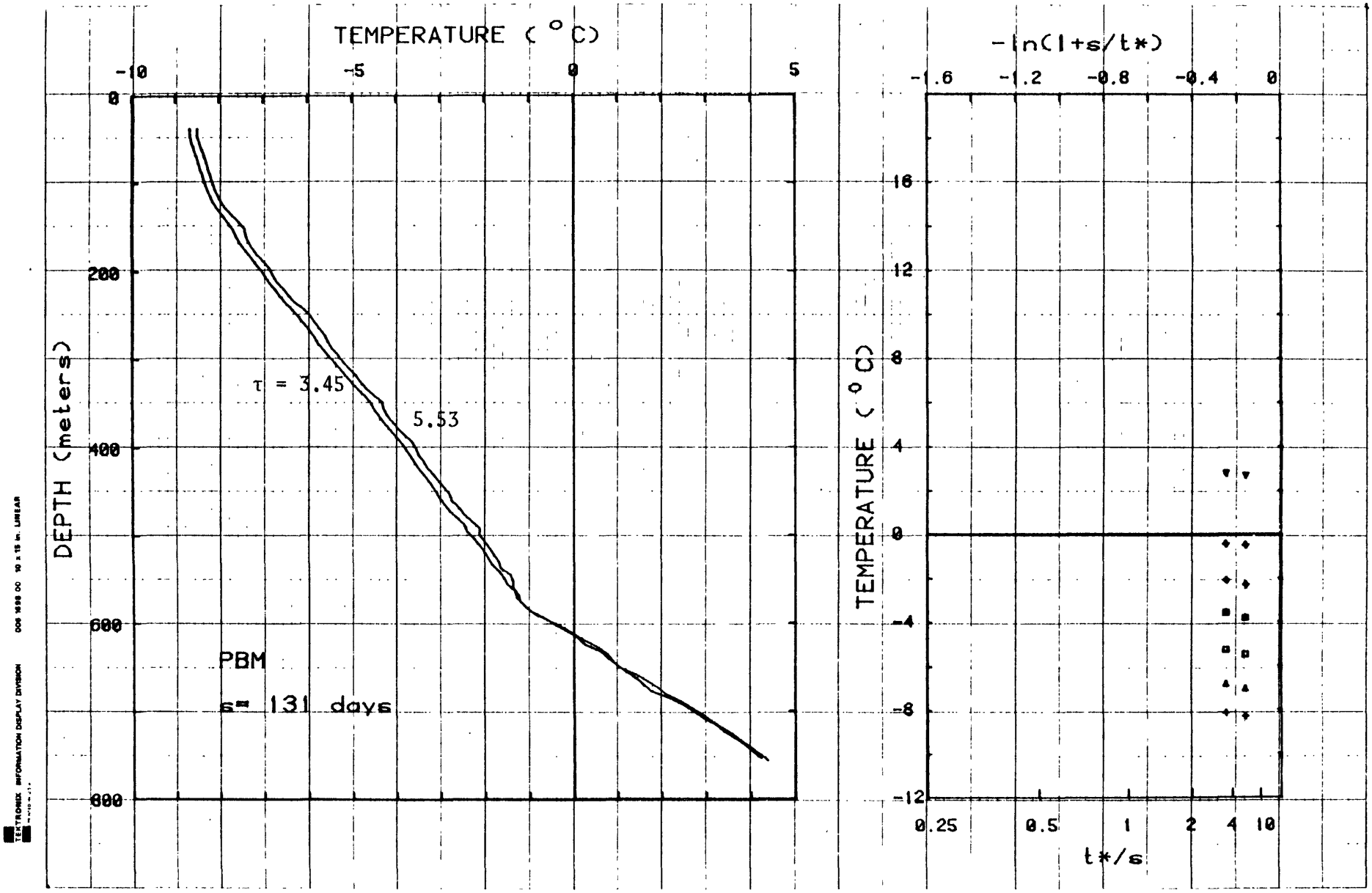
TEMPERATURE (°C)
-10
-5
0
5
DEPTH (meters)
0
200
400
600
800
τ = 3.45
5.53
PBM
s= 131 days
-ln(1+s/t*)
-1.6
-1.2
-0.8
-0.4
0
TEMPERATURE (°C)
16
12
8
4
0
-4
-8
-12
0.25
0.5
1
2
4
10
t*/s

Figure C-13.

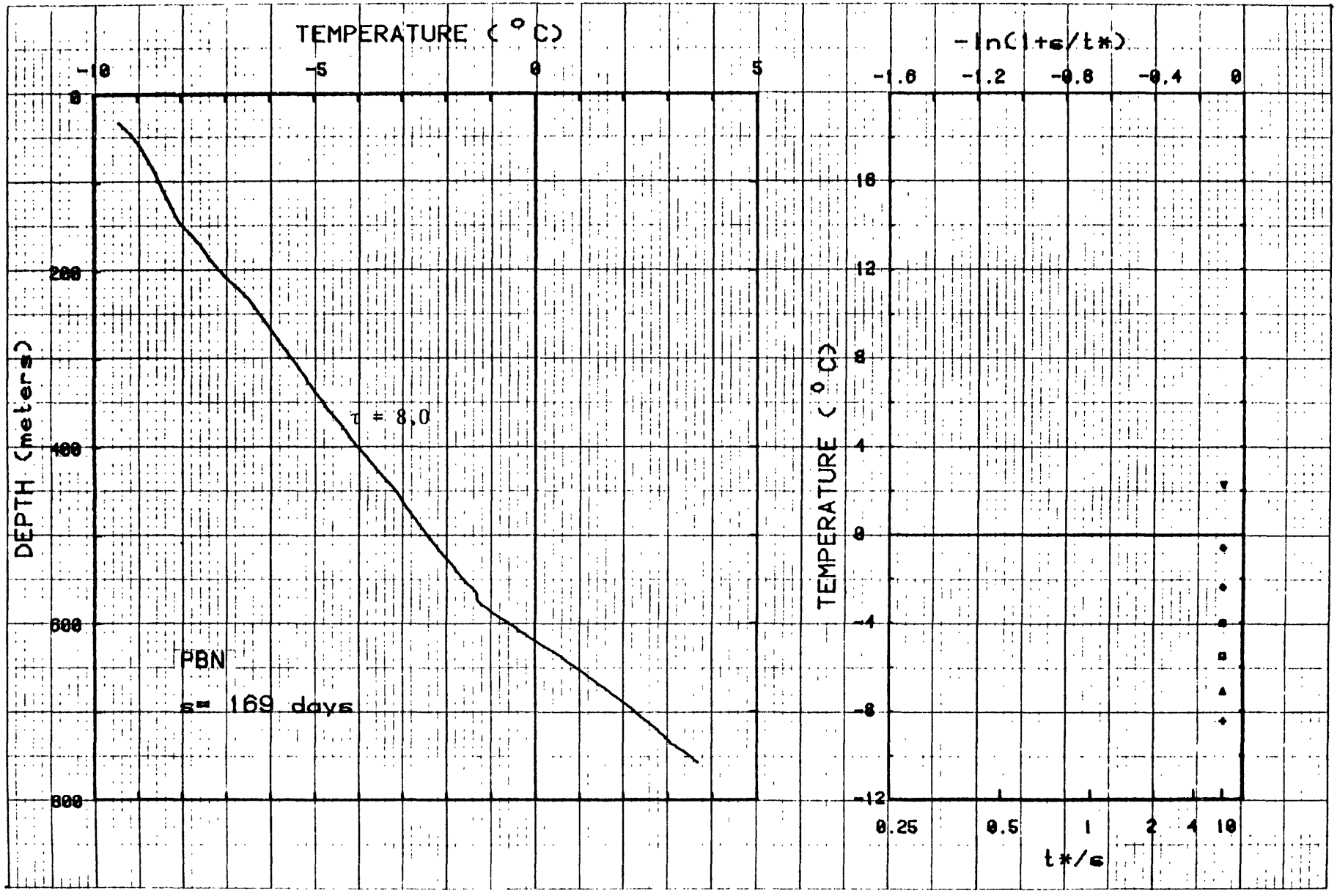
TEMPERATURE (° C)
-10
-5
0
5
DEPTH (meters)
0
200
400
600
800
τ = 8.0
PBN
s= 169 days
-ln(1+s/t*)
-1.6
-1.2
-0.8
-0.4
0
TEMPERATURE (° C)
16
12
8
4
0
-4
-8
-12
0.25
0.5
1
2
4
10
t*/s

Figure C-14.